Janes

Investigation of the airflow in an acoustic jet at resonance.

Thesis
J28

Library
U. S. Naval Postgraduate School
Annapolis, Md.

[illegible]

[illegible]

[illegible]

A Thesis

Submitted in Partial Fulfillment of the Requirements

for the

Master of Science Degree in Agricultural Engineering

at the University of [illegible]

By

Ralph [illegible]

[illegible]

[illegible]

TABLE OF CONTENTS

Summary 1

Introduction 3

Nomenclature . . . . [illegible]

Related Theory . . . . [illegible]

Description of Apparatus and Procedure 13

Results and Discussion . . . . [illegible]

Conclusions 15

Bibliography . . . . [illegible]

16259

LIST OF FIGURES

Figure 1. Principle Apparatus

Figure 2. Mechanical Oscillator

Figure 3. Resonator Open End Modification with "Wall Static" Instrumentation

Figure 4. External Traverse Arrangement

Figure 5. Internal Traverse Arrangement

Figure 6. Resonator Mean Static and Total Pressure Distribution in Axial Direction

Figure 7. Mean Pressure Distribution in Plane Along Resonator Axis of Symmetry

Figure 8. Resonator Wall Static Pressure Distribution for Various Magnitudes of Piston Stroke

Figure 9. Resonator Wall Mean Static Pressure versus Piston Stroke, with Distance from Resonator Open End as a Parameter

Figure 10. Effect of Open End Shape on Mean Static Pressure at the Resonator Surface

Figure 11. Effect of Frequency on Mean Static Pressure at the Resonator Surface for Fixed Resonator Length

Figure 12. Effect of Frequency on Mean Static Pressure at the Resonator Wall for Selected Stations

Figure 13. Determination of Resonant Frequency for Basic Resonator Configuration by Measuring the Mean Static Pressure at the Resonator Surface

Figure 14. Determination of Resonant [illegible] for Tapered Tip Resonator Configuration

Figure 15. [illegible] for Basic Resonator Configuration

Figure 16. External Radial Traverse, Mean Static Pressure

LIST OF FIGURES (cont.)

Figure 17. Mean Pressure Profile at [illegible] Outside of Resonator Open End

Figure 18. Internal Radial Traverse Mean Total Pressure

Figure 19. Dust Figures and Jet at Low Piston Stroke

Figure 20. Dust Ridges Near Open End after Run at a Piston Stroke of 0.502 in.

Figure 21. Dust Figure Leading into Jet at a Piston Stroke of 0.954 in.

Figure 22. Dust Figure Leading into Jet with Smoke Showing Edge Vortices at a Piston Stroke of 0.954 in.

Figure 23. Same as Figure 22 except that Downstream Detail of Jet is More Sharply Outlined

Figure 24. Close-up of Dust Figure; Not visible is the observed fact that these tiny particles are describing straight oscillatory paths parallel to the axis. Dots at the top are six inches apart.

Figure 25. Penetration of Edge Vortex at a Piston Stroke of 0.702 in.

Figure 26. Penetration of Edge Vortex at a Piston Stroke of 0.954 in.

Figure 27. Variation of Depth of Penetration of Resonator, by End Vortex System, with Magnitude of Piston Stroke

Figure 28. Oscillating Particles of Dust Near Resonator Open End (between Stas. 0 and 1) at a Piston Stroke of 0.502 in.

Figure 29. Oscillating Particles of Dust at Same Location as Above but at a Piston Stroke of 0.954 in.

Figure 30. Estimated Dust Particle Path Length for Different Magnitudes of Piston Stroke

Figure 31. Variation of Estimated Dust Particle Path Length with Piston Stroke

Figure 32. Idealized Time-Distance Diagram of Wave Progress in a Resonator Closed at One End by a Pulsator and Open at the Other End

SUMMARY

The airflow phenomenon, known as an "acoustic jet" and associated with an open-end resonator excited by an oscillator, was investigated using a mechanical, piston-type pulsator with piston stroke variable in the range of zero to one inch. The objective was the quantitative examination of the mean pressure distribution by liquid manometer measurements, and the determination of the overall flow patterns and behavior, using flow-visualization techniques.

The work grew out of two recent investigations relating the acoustic phenomenon to dynamic thrust, one of which was done at the United Aircraft Corporation Research Department (Ref. 1), and the other of which was done at the University of Minnesota by R. L. [illegible] (Ref. 2).

Lateral and longitudinal mean pressure gradients are presented for a basic configuration showing the general character of the pressure distribution and the effect of variation of amplitude of pulsating vibration.

The air inside the major portion of the resonator appeared to be pulsating longitudinally without apparent flow or general circulation. An external circulation was evident which

involved a pulsed inflow through an open-edge orifice, an appar-
ent [illegible], and an efflux through a central jet. The penetra-
tion of the end vortex system was found to increase with in-
creased amplitude of piston stroke, but was relatively shallow and
appeared to consist mainly of air which was part of the external
circulation.

The work was carried out in the [illegible] Laboratory of
the Mechanical and Aeronautical Engineering Departments of the
University of Minnesota, under the guidance of Dr. [illegible],
and as a preliminary phase of a much broader investigation to be
performed by the University with United Aircraft Research Depart-
ment support.

INTRODUCTION

Many phenomena encountered in the jet propulsion field remain obscure and little understood. Among the foremost of the problems requiring further analysis and investigation are those relating to intermittent and pulsating gas flow. Resonance phenomena are utilized to regulate the gas flow in the pulse-jet. The airflow phenomenon known as the "acoustic jet" is associated with various configurations of tubes or resonators, closed at one end, and excited by a pulsator. Interest has been heightened by the long established fact that under certain conditions a significant amount of thrust is produced by these simple devices with only a small input of energy to the pulsator. Further, engineers testing jet engines have sometimes observed performance improvement associated with resonance.

A comprehensive summary of the historical background, basic acoustic theory, and the nature of early investigations in this field, has been given by Streiter /2/ as part of his report relating the acoustic phenomena directly to acoustic thrust. Other recent investigations include that at Cornell Aeronautical Laboratory (CAL) (Refs. [illegible]), United Aircraft (Ref. [illegible]). Although significant mathematical treatments of wave propagation in tubes of this nature are available (Rayleigh /3/, [illegible] /[illegible]/

LeVart /13/, Wood /9/, Morse /4/, and Refs 5, 6, 7), it appears that further analysis and investigation is needed in the case of the acoustic jet.

Previous investigations (Refs. 1, 2) have concentrated largely on directly relating the acoustic phenomena to thrust and have shown among other things that the acoustic jet driving is extremely sensitive to open-end edge conditions, and that it is possible to increase the thrust by increasing the amplitude of the forcing vibration. A broad program of further quantitative and qualitative determination of the flow fields in acoustic jets is needed for the attainment of adequate understanding of this special problem and for further insight into the general characteristics of pulsating flow. Pressure surveys, paralleling the thrust investigations, are needed.

A mechanical pulsator was designed and built by the University of Minnesota Mechanical Engineering staff for use in a broad program of research in pulsating phenomena employing both mean and instantaneous observations. This program was made feasible by United Aircraft Research Department support. The pulsator was kindly made available for the present work which was proposed as a preliminary phase of the broad program.

The primary objectives were twofold; (1) verification

of the flow patterns and behavior employing tufts, smoke, and dust as flow visualization techniques, and thus establishing, if possible, the salient characteristics of the flow associated with the basic resonator configuration in the available range of amplitude of pulsator vibration; (2) obtaining mean static and total pressure data, using liquid manometer measurements, showing mean pressure distribution in the basic resonator and jet excited by the highest available (about one inch) amplitude of pulsator vibration.

The work was carried out in the Engines Laboratory of the Mechanical and Aeronautical Engineering Departments of the University of Minnesota, under the guidance of Dr. N. A. Hall. The author wishes to express his appreciation for the use of the pulsator, which was made possible through United Aircraft Research Department support, and to express his thanks and appreciation to the following: Dr. N. A. Hall, for his direction and counsel; Professor P. M. Murphy, for his suggestions; Ass't. Professor E. L. Kelly, for his suggestions and assistance.

NOMENCLATURE

h_s — Gage mean static pressure, inches of water, referred to atmospheric pressure.

h_o — Gage mean total pressure, inches of water, referred to atmospheric pressure.

H_a — Ambient atmospheric pressure, inches of mercury, absolute.

t — Ambient atmospheric temperature, degrees Fahrenheit. Also used for time in seconds.

T — Absolute temperature, degrees Rankine. Thrust in lbs.

X — Distance along resonator axis, in inches, measured from the plane normal to the axis, at the open end of the resonator, towards the closed end (piston).

$-X$ — Same as X except measured in the other direction (external).

x — General variable for distance along resonator measured from plane of closed end.

L — Resonator length in inches.

ϕ — Angular position in degrees in any plane normal to the resonator axis; referred to a zero line extending from the axis vertically upward, and increasing in a clockwise direction as the observer faces the closed resonator end from the open end. This is used in the Tables (see Table VII and subsequent tables through XII) to indicate the circumferential direction of the probe at the introduction point. Thus, in Table VII, the static wall pressure at the probe introduction point is at the top of the pressure data column for 0° and for 90°, and is at the bottom of the pressure data column for 180° and for 270°.

r — Radial distance from the resonator axis in inches, positive along the line defining ϕ; negative along the line defining ϕ + 180°.

r^1 — Distance, in inches, measured from the inside resonator wall along a line extending through, and normal to, the resonator axis. Thus it has its largest magnitude at the resonator axis. It is not used negatively.

RPM & N — Revolutions per minute of the pulsator crankshaft unless reference is to some other mechanism.

S — Piston stroke in inches measured from head-end dead center.

R — Crank radius in inches.

L — Center to center length of connecting rod in inches.

θ — Angular position of the pulsator crank from head-end dead center.

V — General velocity variable.

u — Velocity paralleling resonator axis, positive in direction of positive x.

a — Speed of propagation of a sound wave.

f — Frequency, cycles per second.

ω — Angular velocity, radians per second.

Terms Used in Tables

Basic Resonator Configuration. Refers to the basic resonator configuration as described in detail under Apparatus.

Wall Static. Refers to the instrumentation arrangement described, and so referred to, in the section on Apparatus.

Internal Traverse. Refers to the instrumentation arrangement described, and so referred to, in the section on Apparatus.

External Traverse. Refers to the instrumentation arrangement described, and so referred to, in the section on Apparatus.

<u>Square</u>. Used with reference to the open end edge of the resonator, it signifies that the tube was cut squarely off in a plane normal to the axis and that the resulting edge was not modified by tapering.

<u>Sharp</u>. Used with reference to the open end edge of the resonator, it signifies that the edge was tapered to a sharp edge coincident with the end of the inner wall.

RELATED THEORY

The elementary theory, concerning the possible resonant modes of vibration in air columns traversed by plane pressure waves or impulses, is well established and appears in most text-books on sound (Refs. 7, 8). It should suffice to review briefly the theory directly related to the resonator configuration which was used in this work, namely, a circular tube open at one end and closed at the other.

Single Resonator Theory

Pressure impulses produced in a tube by plane surfaces normal to the axis are generally assumed to propagate as plane pulses or waves. These waves reflect where area discontinuities occur. Upon encountering a plane wall, as a closed end of a tube, they reflect without a change of phase. Upon encountering an "openness", as at the open end of a tube, they reflect with a one-hundred eighty degree change of phase, i.e., compression waves are reflected as expansion waves and expansion waves are reflected as compression waves. These waves travel at local sonic velocity or higher with respect to the air particles and depending upon their strength. When the tube length and frequency of pulsation are related in such a way that reflected waves return

at the origin just as a [illegible] of the same phase is starting, reinforcement occurs, the waves have greatly increased strength, and it is said that the tube is resonating.

The wave length is four times the distance between a node and the adjacent antinode since the antinode corresponds to a point of instantaneous one-hundred eighty degree change of phase. Thus there must always be an antinode at the open end of a resonating tube and a node at the closed end. From these considerations it is easy to deduce the resonant wave length, period, and frequency. For the tube closed at one end and open at the other, we follow the progress of a compression wave through a complete cycle. A compression wave is started at the closed end, reflected at the open end as a rarefaction, reflected again from the closed end as a rarefaction, and finally from the open end as a compression which returns to the origin after having traveled four times the length of the tube. This is the fundamental mode of vibration for this tube configuration. The wave length is therefore 4L, the period is 4L/c, and the frequency is c/4L. The harmonics would occur at higher frequencies of 3c/4L, 5c/4L, etc.

[illegible]

experiment that an "end correction" is needed. Thus, the generally accepted formula for the fundamental frequency of such a resonator is (ref. 1).

$$f = c/4(L + 0.6r) \qquad (1)$$

<u>Idealized Time-Distance Diagram</u>

Carrying along the assumptions inherent in the simple theory given above, and adding the additional assumption that the compressions and rarefactions are weak plane waves produced instantaneously at the mid-stroke position of the piston, it is of interest to follow the progress of these compressions and rarefactions in an idealized time-distance diagram ("t-x" diagram) such as is shown in Figure 2. The small arrows indicate the direction of the velocity increments following, and impelled by, the waves. The circled numbers indicate that the strength of the wave is still [illegible]. Physically, bringing all losses [illegible] into the actual situation is that a state of equilibrium is reached when the energy input of the piston is balanced with the losses, and at that point the waves have reached their maximum strength.

Piston Motion

The motion of the piston is of interest because it originates the pulses and determines the boundary conditions at the closed end. The pulsator employed in this investigation was designed with a conventional crank-pin and connecting rod linkage with provision for adjusting the piston stroke in the range of zero to one inch. Thus (Ref. 10), the piston displacement from head-end dead center (X) is:

$$X = L + R - (L^2 - R^2 \sin^2 \theta)^{\frac{1}{2}} - R \cos \theta \qquad (2)$$

where L is the center-to-center length of the connecting rod; R is the crank radius; and θ is the angular position of the crank from head-end dead center. The approximate piston velocity (V) in feet per second is:

$$V = [illegible]\,NR(\sin \theta + \tfrac{1}{2}\lambda \sin 2\theta) \qquad (3)$$

where N is rpm; R is in inches; and $\lambda = R/L$. The approximate acceleration of the piston velocity (A) in feet per sec.^{2} is:

$$A = [illegible]\,N^2R(\cos \theta + \lambda \cos 2\theta) \qquad (4)$$

where the units are as before.

Additional Wave Theory

Reinforcement of a cumulative nature is taking place at resonance, so that the final level of pulse strength is difficult to predict. If the coordinates are transferred to the disturbance front, it is evident that the approach velocity of the flow relative to the traveling pulse is never less than sonic and may be somewhat greater depending upon what the final level of pulse strength and temperature distribution actually is. It is shown in aerodynamics texts that the local velocity of wave propagation is a function of the local absolute temperature, thus (Ref. 16):

$$a = \sqrt{g \gamma R T} = \sqrt{\gamma P/\rho} \qquad (5)$$

where the units must be consistent.

There are certain fundamental physical differences between compressive waves and expansive waves. Some of these are ordinarily considered negligible when treating small-scaled waves, but are by no means so when dealing with strong waves or the conditions produced by the repetitive passage of a great many weak waves. It may be shown (Ref. 15) that if a finite, continuous, <u>compressive</u> wave be started, such as by a piston moving rapidly in a tube, each point of this disturbance, though it

of it a small step wave, each propagates itself at the local speed of sound, relative to the fluid at that point, and will therefore overtake the initial increment of the wave, after a finite time, to form a discontinuity such that the compression takes place practically instantaneously. This must occur because the pulse of a compression wave is characterized by an increase in entropy and temperature (and thus velocity of propagation) over the approach conditions. The time necessary for this to occur is given as (Ref. 17, p. 47).

$$t = (2/\gamma + 1)\ (1/m) \qquad (6)$$

where $m = (du/dx)_{max}$, the maximum slope of the impressed velocity-distance curve. If the maximum slope of the velocity-distance curve for the piston be taken as a crude approximation of that value, one finds, for the case of one-inch piston stroke and 1005 RPM related to a nine foot long resonator, that the time required to form a discontinuity would be approximately 0.050 seconds, while the time required for the pulse to reach the open end of the resonator would be approximately 0.008 seconds so that a discontinuity is not formed. Only if the reinforcement reached the point where the actual slope of the velocity-distance curve for the flow near the piston was six or seven times the value for the piston, [illegible]

would appear near the open end of the resonator.

The reverse situation is true for an expansion wave. Each succeeding increment of such a wave finds itself travelling in a slightly cooler medium than the increment which preceded it, and thus at a slightly lower rate. Thus expansion waves tend to become less steep and to spread out. There is no natural mechanism for the formation of a discontinuous expansion wave (Ref. 18). The approach flow velocity relative to an expansion wave receives an increment of velocity increase, whereas compressive waves impart a decrement.

Measurement of Oscillatory Pressures

Special problems arise in connection with the simplest measurements of oscillating pressures. The fluid is alternately flowing in and then out of the measurement transmission system and this is a non-isentropic process involving flow work and accompanying pressure losses. The natural frequency of the instrumentation, if excited, may completely distort the actual picture. The main factors are therefore: attenuation, resonance, and lag.

Attenuation refers to the pressure drop along a tube due to viscous forces (not resonance effects) and is generally calculated on the basis of Poiseuille's law of viscous flow through

which is given as (Ref. 11):

$$\partial p/\partial x = -(128/\pi)(\mu_0/D^4)Q \qquad (13)$$

where p is the instantaneous pressure at any point in the connecting tube; x is the distance along the tube measured from the entrance; μ_0 is the mean fluid viscosity; D is the tube diameter; Q is the volumetric flow at any point in the tube. Equation (13) is combined with the non-steady, one-dimensional form of the equation of continuity, in Ref. 11, to obtain a solution for values of the loss in ratio of amplitude of pressure for instantaneous pressure measurement devices. Sinusoidal variation of the entrance is assumed (about the mean pressure), and it is assumed that the instrumentation has been design so as to avoid acoustic resonance effects.

An earlier work (Ref. 12) offers a solution which approximates the variation with time, and is perhaps more suited to estimation of the attenuating effect on mean pressure measurements.

In this case, equation (13) was integrated directly, assuming constant volume flow per unit time, Q, giving, for laminar flow ($0 \le Re \le 2000$).

$$p_1 - p_2 = (128Q\mu/\pi D^4)L \qquad (1[illegible])$$

and for turbulent flow (2000 ≤ Re ≤ 100,000),

$$p_1 - p_2 = 1/6\,(4/\pi)^{7/4}\,\left(\frac{\mu^{1/4}}{\rho_0}\right)\left(\frac{Q^{7/4}}{D^{19/4}}\right) L \qquad (17)$$

where the units used are consistent, Q is the mass rate of flow, and the pressures p are mean values at the entrance and sending end respectively. A criterion for determining the type of flow was given as a condition for laminar flow, where the critical Reynolds number was taken as 2000. Thus,

$$D^5\,\Delta_p/L < 3.4 \times 10^{-8} \qquad (18)$$

for laminar flow, where D is in inches and Δ_p/L is pressure drop in inches of mercury per foot of tubing.

<u>Distortion</u> is the ratio of the value of the pressure at the measuring element to the corresponding value at the entrance of the transmission line. Thus, if the attenuation were zero, the pressure ratio would be just the effect of natural frequency oscillation in the measuring device. This is given particular attention in NACA TN 1119 (Ref. 12). The electrical analogy is used. The cases of systems with and without negligible instrument volume are treated, as well as amplitude characteristics of systems having a periodic pulsation. No theoretical method of predicting the attenuation characteristics of the tubing is given.

The *leg* is the [illegible] [illegible] [illegible] [illegible] the system [illegible] [illegible] [illegible]. [illegible] [illegible] [illegible] [illegible] [illegible] and [illegible]. 11.

DESCRIPTION OF APPARATUS AND PROCEDURE

The principal apparatus in this investigation consisted of the mechanical pulsator which could be adjusted to various stroke amplitudes, the resonator, flame chamber, manometers, various probes, apparatus for producing sound and introducing coal and dust, special lighting, and a variable-speed DC generator as a power source.

The power source (see Figure 2) was a portable welder, direct current, laboratory test type, Electric Specialties which had ratings: rpm, [illegible]/1500; HP, 15/20; amps., 125; volts, 250.

The mechanical pulsator (see Figure 1) was designed and built by the University of Minnesota Mechanical Engineering Shops with the support of the [illegible] Department. A small flywheel was splined to a shaft that was direct coupled to the generator and mounted in two bearings. A crank pin projected from a small, circular plate which was bolted to the flywheel with two bolts. Taking advantage of the properties of an ellipse, a pattern of holes was made in the flywheel such that it was only necessary to put the two bolts in a different pair of holes to change the crank radius and thus the

piston stroke. Four eccentric holes in the flywheel permit eight possible piston stroke magnitudes available in the range of 1.00 to [illegible] inch. The values of piston stroke used in this investigation were, in inches: (0.274, 0.446, 0.611, 0.785, 0.97[illegible]). These values included the minimum and the maximum for the apparatus. A needle pin bearing connecting rod (five in. long, center to center) was connected to a thrust shaft. The thrust shaft was provided with a guide bearing. The piston screwed on to the head end of the thrust shaft and fitted into a steel cylinder mounted in an oak frame. The piston, connecting rod, thrust shaft, and guide bearing were all of aluminum. The piston had about two thousandths clearance in the cylinder when cold, and had no provision for sealing except the thermal expansion of the aluminum when hot. The cylinder was five and one-half inches in diameter (corresponding to the inside diameter of the resonator) and eight inches long. The head end two inches of the cylinder was widened to six inches to receive the resonator tubing.

The basic resonator configuration, as the term is used in the text and tables, refers to the resonator configuration as described in this paragraph. Two sections of cylindrical, plastic tubing (32.[illegible] inches long; 6.0 inches O.D., 5.5 inches I.D.) were butted together and cradled horizontally in three wooden supports

(see Figure 1). One end was inserted in the pulsator receiver station. The butted ends were sealed with Scotch tape which was easily removable. Small patches of the same material were used to seal orifices which were not in use. The overall length of the resonator, measured from the open end to the mean piston position (one-inch stroke), was found to be one hundred seven and four-tenths inches, or nearly nine feet. The plastic tube ends were square-cut, and in particular, the edge of the open end of the resonator was square-cut or sharp. Eighteen orifices (0.070 in., drilled with sharp No. 50 drill) were spaced six inches apart, in a straight line along the upper surface. These were numbered as stations one through eighteen starting at the open end. The orifice near the open end was set in from the tube end by about 3/16 inches to permit attachment of fittings. Three additional orifices of the same diameter were drilled at stations 2, 7, 12, and 17. These, together with the top orifice, were given equidistant angular spacing (90° apart). The tube was carefully aligned with the axis of the pulsator piston. The resonator open end was eight feet from the facing wall and the resonator center axis was thirty-four inches from the floor.

The main modification to the basic resonator configuration, considered in this work, was the attempt to investigate the effect of a sharp versus a flared open-end edge (Figure 5). This

was done by making a cylindrical tin collar two and one-half inches long which fit snugly inside the open end of the [illegible]-tor. It was inserted one-half inch into the open end, which increased the resonator length by two inches. Modeling clay was then applied to the outside of the tin collar to produce first the sharp, and then the blunt, open-end edge configuration. A pressure tap near the edge of the tin collar was numbered as station 1a. A similar tin collar was used at the intersection of the tube sections for some flow visualization runs (Figure 10). It fit over the outside of the tubes and was one and one-half inches long so that it increased the tube length by one-half inch. It had one hole to admit a 3/16 inch OD probe, and another to admit a one-half inch [illegible] spout. These holes were sealed with Scotch Tape when not in use.

Two identical plenum chambers were built (see Figures 1, 2). They were made from four inch galvanized rain spout and were fifty-six inches long. One of the [illegible] was flattened to permit the soldering on of flat plates (one-fourth inch thick), which were spaced [illegible] inches apart and tapped to receive ordinary one-eighth inch pipe [illegible] fittings. A similar fitting was attached at each end. Rubber tubing (one-fourth inch ID, approximately thirty five inches long) was attached to each of the end fittings and connected to a T fitting,

(5/16 inch ID). Similar pieces of rubber tubing, approximately fifty-five inches long, were used in connecting the two Y fittings to liquid manometers when the plenum chamber only [illegible].

The manometers employed were of the liquid, draft gage type (Figure 1). The one which was used for all the traverse readings and with the plenum chamber [illegible] during the wall static measurements was a laboratory [illegible]. The scale was calibrated, however, in inches of water. The range was zero to fifteen inches with only the zero to three inch part of the scale inclined. A small three inch-scale, draft manometer (inclined), filled with distilled water, was used with the plenum chamber outside the operator, except for occasional readings at Sta. No. 1 which were off the scale. These manometers could be read to the third decimal place on the inclined scale and to the second decimal place on the vertical scale. All readings were taken as referring to atmospheric.

The pressure measurement instrumentation was of three types: (1) wall static, used for most of the measurements of mean static pressure at the diffuser wall; (2) internal traverse, used for the mean static and total head pressure traverse measurements inside the diffuser; (3) external traverse, used for traverse measurements in the jet.

The ball [illegible] configuration (Figures 2, 3) consisted of the two plasma discharge and associated hardware as shown in Figure 3. The plasma chamber or resonator [illegible] copper tub-ing. A small [illegible] was fitted over a piece of copper tubing [illegible] to the same curvature as the outside of the resonator and was one inch long. [illegible] of the [illegible] and three-quarters inches wide. The copper tubing was one and one-half inches long, five-sixteenths inches OD, and three-eighths inches ID. The stop-cock fitted to the [illegible] had a straight, [illegible] bore, [illegible], of [illegible] inches inside [illegible]. [illegible] end of the stop-cock had an external [illegible] similar to a ball-joint, so that it [illegible] could be [illegible] by [illegible] of rubber [illegible]. The [illegible] was [illegible] a rubber gasket and a metal clamp [illegible]. The [illegible] the copper tube was connected to the resonator by a piece of rubber tube [illegible] inches long [illegible] ID. [illegible] between the resonator and the base fitting was approximately one-half inch [illegible] the plasma was in position, [illegible] [illegible] [illegible] of the copper tube. [illegible]

chamber was about three and three-fourths inches with three dif-
ferent changes in boundary, namely, the rectangular fitting, the [illegible] entrance connection fitting, and the [illegible].

A modification of the brass seal fitting configuration was made at the [illegible] as shown in Figure [illegible]. This was done to permit the [illegible] connection needed in the [illegible] of the opening condition, and to eliminate the wall effect of the long tube fitting used in the glass [illegible]. The [illegible], in this case, consisted of two short lengths of brass tubing which were soldered on concentric plates so that they were flush with the inside of the pressure wall. This brass tubing had an inside diameter of thirty-three thousandths, and an outside diameter of sixty-three thousandths. A similar piece of brass tubing was [illegible] in place of the [illegible] of the glass chamber. [illegible] of plastic, [illegible] tube length [illegible]. The [illegible] of the [illegible] [illegible] is [illegible] in Figure [illegible].

[illegible] internal [illegible] [illegible]

rangement as shown in Figure 9. A metal base plate, metal clamp, and rubber gasket were used to attach the fitting to the protractor as shown. A brass fitting, normally used to attach copper tubing with a flared end to a needle valve (Imperial 3/8 fitting), was modified by filling the inside hole with brass and drilling two holes to the dimension required for the probe it was desired to use. The cross-cut for this fitting was a small, six-inch, steel scale (calibrated to sixty-fourths of an inch) mounted on its side and extending in a direction normal to the protractor surface. The cut also made a small rubber washer inside it to provide an air seal at the probe. The probes were connected to the mercury manometer on the plenum chamber by a six-inch piece of plastic tubing, carrying the tubes inside the chamber. The various probes used with this arrangement are described subsequently.

A description of the probes used with the internal traverse arrangement follows.

(1) A probe for the approximate measurement of static pressure was made from a hypodermic needle. The end was cut off squarely and polished so that if the probe axis were exactly normal to the flow direction, the flat end plane would be parallel to the flow and a static pressure reading would

be obtained. This probe was [illegible] inches long, twenty-two thousandths inches ID, and [illegible] thousandths inches OD.

(2) Another static probe similar to (1) was made from brass tubing. This probe was eight and one-half inches long, thirty-two thousandths inches ID, and sixty-three thousandths inches OD.

(3) A total head probe was made from brass tubing with the same dimensions as (2) except that it was nine inches in length, overall. The end of this probe was again rounded to hemispheric shape, except that the end remained open. A one-eighth inch radius ninety-degree, bend was made one and one-half inches from the end so that the plane of the opening was approximately one-half inch displaced from, and parallel to, the axis of the major portion of the probe. This will be referred to as the L-shaped total head probe because of its shape.

(4) A total head probe was made from brass tubing with the same dimensions as (2). In this case, the end was closed off with solder and polished down to the shape of a hemisphere. A hole was drilled in

the side of the probe three-sixteenths of an inch from the end. This hole was twenty-eight thousandths (0.028 in.) diameter which was only slightly different than the inside diameter of the probe (thirty-three thousandths). This probe has been referred to as a cylinder-type total head tube since it is based on the fact that stagnation occurs at the leading edge of a cylinder placed normal to a steady flow.

The _external traverse_ configuration consisted of an arrangement as shown in Figure 8. The probe fitted snugly into a one inch bearing in a mounting plate on the support frame. It could be slid back and forth using a scribed scale calibration on the probe for positioning. Vertical positioning could be made by moving the mounting plate up and down between the two vertical support bars. When positioned vertically, the mounting plate position was fixed by a clamp arrangement. The vertical support bars could be rotated about a vertical axis providing another degree of freedom. The external traverse probes were connected to the plenum chamber by a six-inch piece of rubber tubing (3/16 in. ID) and a one-way stop-cock.

A description of the _probes_ used with the _internal traverse_ arrangement follows.

(a) A Kiel (total-head) tube (Ref. 14) with a shielded [illegible] was available and this was used for all of the external total-head measurements. The sensing tube inside the outer shell of this probe had an inside diameter of approximately [illegible] of an inch and was approximately two inches in length. It led into a larger brass tube which also served as the support or probe shaft, the orientation of the Kiel tube being at a right angle to the shaft axis. The shaft was eighteen inches long, making about twenty inches overall, five thirty-seconds of an inch in inside diameter and three sixteenths of an inch outside diameter. The outer shell of the Kiel tube was one-quarter inch in outside diameter and its head end was offset from the axis of the shaft by three-eighths of an inch.

(b) A static probe for use with the external survey arrangement was made, from brass tubing, into the shape of an L, where the short part was four inches long and the long part, which served as the probe shaft, was eighteen inches long. The shaft had the same dimensions as the shaft of the Kiel

tube (C), but this was reduced at a point two inches short of the bend. From here on the smaller section of the tube was six inches in overall length, one-eighth of an inch in inside diameter. The end of the short part of the "L" was cut square and polished smooth so that, if its plane were placed exactly parallel to the flow, it would read nearly the static pressure. It was used in this way, facing down, with the end plane lying in the horizontal plane of symmetry through the central axis of the generator and jet.

Various methods of producing smoke were tried. The most satisfactory method employed [illegible].

Quantities of a white, plastic, siliceous, insulating material, with the trade name Santocel (Monsanto Chemical Company), were available. This material is extremely light, with a fluffy, cotton-like texture. The finest particles have a very low free-fall rate. This was injected into the generator at the air-shaft by blowing it through a large funnel, or by simply sprinkling a little along inside the tubes before the start of a run.

The flow pictures shown were taken using a [illegible]

light [illegible] with a fibre-glass jacket. [illegible] was produced by [illegible] with a [illegible].

[illegible] but [illegible] general recommendations [illegible] pulsating flow measurements contained in an [illegible] /15/. [illegible] concluded that "the first resonant frequency of the pressure-measurement system should be kept well above the highest pressure frequency to be measured. This should be ideally be accomplished only by installing the pressure-sensing element as close to the point of measurement as possible." Thus, tube length for pulsating pressure measurements must be kept as short as possible. With a liquid connected to the sensing instrument, [illegible] can be used to dampen the pulsations.

RESULTS AND DISCUSSION

Mean Static and Total Pressure Distribution Along the Resonator Axis of Symmetry

Values of mean static pressure, mean total pressure taken with the probe opening facing the piston, and mean total pressure taken with the probe opening facing away from the piston, [illegible] in Figure [illegible] for [illegible] inches. [illegible] values occur near the piston and the lowest values [illegible] just inside the resonator mouth. All values [illegible] of the resonator, [illegible], referred to atmospheric, [illegible] steadily [illegible] outside the resonator.

The total [illegible] in opposite directions, parallel to the axis, [illegible] little difference in the region near the piston (Figure [illegible]). A tendency for the "facing-away" readings to [illegible] the "facing" readings [illegible] toward the resonator open end. At a [illegible] inches inside the resonator, this trend is [illegible], [illegible] divergence at the open end. [illegible] just outside the resonator open end [illegible] flow with the total head facing the piston [illegible] [illegible] on the total head facing away from the [illegible] [illegible] static values of the [illegible].

with increased external distance from the open end of the resonator.

The reversal of dominant total head values at the resonator mouth suggests that the air inflow and outflow is truly alternating over the whole open end, and that the air coming in has nearly atmospheric total pressure, since it is mostly drawn from the surrounding atmosphere at the inlet, and has experienced the dissipation associated with intense oscillations over a relatively short time. Rayleigh /[illegible]/ states, "the two effects (inflow and efflux of the air in a jet) are of course in reality alternating, and only appear to be simultaneous in consequence of the inability of the eye to follow such rapid changes".

The total head reversal, at a short axial distance [illegible] inside the resonator open end, marks the transition point between the phenomenon inside the major portion of the resonator which appears to be primarily oscillatory, and the end vortex and jet flow which appears to be primarily an external circulation system strongly located in the region of the resonator open end. Visual observations (Figure [illegible]) suggested that much of the surrounding air, drawn towards the resonator open end, joined the jet flow from the periphery of the vortex system without

entering the resonator. It appears that this air has [illegible] momentum and turbulence throughout the jet flow.

The maximum difference between static and total head values (approximately three and one-half inches of water) occurs just inside the resonator open end and are indicative of velocities of the order of one hundred twenty-five feet per second. The mean velocity at one foot outside the resonator is indicated as about eighty feet per second, and the mean velocity at a distance of three feet outside the resonator is indicated as about sixty feet per second. These values compare with the maximum instantaneous piston velocity of eight and one-tenth feet per second for the 0.278 in. piston stroke.

Lateral Pressure Gradients

A comparison of the mean static pressure distribution along the wall of the resonator with the axial mean static pressure distribution is shown in Figure 8. The axial gradient is greater than the wall gradient and shows considerably lower pressure values than along the wall as the open end of the resonator is approached. The values are very nearly the same near the closed end. A sharp reversal of the static pressure trend occurs just inside the open end, which may be related to the effect of the edge vortex system. The divergence of the

axial and wall static pressure distributions correlates with the visual observations of greatly increased dust particle path lengths near the open end, assuming that the latter are an indication of increased gas molecule path lengths.

Profiles of mean static pressure distribution inside the resonator are shown in Figures   16. These profiles, with the exception of that for station One, were obtained by probing from two pairs of opposed directions at each station as a check upon the symmetry of the pressure distribution.

Profiles of mean static and total pressures in the external jet area (horizontal plane) are presented in Figure 17 for distances one-half, two and one-half, and six inches from the open end of the resonator.

Total head profiles are presented in Figure 18. Their gradients appear to be small except in the region near the open end of the resonator.

Variation in Mean Static Pressure Distribution with Piston Stroke

The mean static pressure distribution along the resonator wall for various magnitudes of piston stroke is shown in Figure 9. The pressure gradient is greatly reduced with piston stroke, although the original pressure distribution pattern is

retained. The cross plot of pressure versus piston stroke is shown in Figure 9. It appears that the variation is essentially linear in this range. This agrees with the tests of the [illegible] versus piston stroke results presented in Ref. 1 for a straight resonator without end modification. The greatest rate of change is positive and is near the closed end, and the least rate of change is negative and is near the open end.

Variation in Pressure for a Flared and Sharp-Edged Open-end Resonator Configuration

The difference in wall static mean pressure distribution for resonators with flared and sharp edged open-end resonator configurations is shown in Figure 10. Somewhat lower values were obtained with the tapered edge.

Variation in Wall Mean Static Pressures with Frequency for Fixed Resonator Length

The variation of mean static pressure distribution along the resonator wall is shown in Figure 11 for various pulsator [illegible] values. A cross plot of pressure versus [illegible] for selected stations is shown in Figure 12. It is evident that a longitudinal pressure gradient is produced which [illegible] the resonator

[illegible] of the resonant frequency; and that this gradient is such that the minimum tends to occur at, or near, the closed end (piston). The higher values occur at, or near, the open end. This is in agreement with theory (Ref. 7). Response [illegible] had [illegible] to determine the resonant frequency of the basic standard configuration in Figure 13, and for the open-end [illegible] modification in Figure 14. The resonant [illegible] for the basic configuration was taken as 1405, and resonant [illegible] for the [illegible] configuration was taken as [illegible]. The theoretical formula (Equation 1) gave values of [illegible] and [illegible], respectively.

The [illegible] curves show a definite difference in the slope on either side of the peak. The positive slope flattens out as resonance is approached while the negative slope drops off much more rapidly. A jump [illegible] at the peak reflects the instability [illegible] with the [illegible] in this range. [illegible] operating [illegible] the peak [illegible]. It may be noted that the general shape of the [illegible] frequency curves, [illegible], is [illegible] the [illegible] of the highest [illegible] pressure [illegible] in this manner.

Thrust Values

Using the mean static pressure values from [illegible], and assuming that the outside pressure on the piston was atmospheric, values of thrust were calculated for various values of piston stroke. These values are plotted in Figure 18. [illegible] shown in Figure 6. [illegible], Ref. 1, [illegible].

The maximum value of thrust calculated [illegible] for the piston stroke of [illegible] in. and the long extension of length [illegible] in. [illegible]. The value for [illegible] in. [illegible]. This compares [illegible] value of thrust [illegible] similar [illegible] (Ref. 1), [illegible] tubes.

Visible Aspects of [illegible]

The [illegible] figures (Figure 10), [illegible] described by early investigators ([illegible]), were [illegible] (0.054 in.). It became [illegible] difficult to produce the [illegible]

figures with increased piston stroke up to one inch. However, with the introduction of sufficient quantities of [illegible], the [illegible] large, [illegible] figure [illegible] [illegible] [illegible]. This large figure would [illegible] affected by [illegible] the [illegible] jet [illegible]. [illegible], however, [illegible] change in spacing. The [illegible] became lower and more irregular (Figure 20) with increased piston stroke magnitude.

Diffusion of [illegible] small quantities of [illegible] was extremely rapid at large strokes of piston motion making detail observation difficult, [illegible] to be associated with large pulsation amplitudes. The distribution of large quantities of [illegible], introduced directly [illegible], appeared to be by [illegible] diffusion at [illegible] greater rate associated with the [illegible] present, and apparently [illegible] pattern of [illegible] circulation within the [illegible] as [illegible] suggested ([illegible] /6/). [illegible] circulation [illegible] associated with the jet flow, but this effect appeared to be [illegible] with only relatively [illegible] primary penetration of the [illegible] as shown in Figure 22 for [illegible] piston stroke amplitude.

A comparison of the depth of penetration of the end vortex system with small and large piston stroke magnitudes is presented in Figure 26 [illegible]. The estimated increase in penetration with increased piston stroke magnitude is plotted in Figure 27 from these and other observations.

Small particle oscillation or vibrating back and forth in a straight line appear to be [illegible] straight lines if the pulsation is fast enough. The observation of fine, individual, suspended particles of dust or lint inside the combustor was quite readily made. The best observations were possible when only a few, fine particles were present so that interference between particles was negligible. The dust particles described straight paths which were usually parallel to the axis throughout the combustor, including the small portion penetrated by the jet vortex system. The location of these particle paths seemed to be stationary, with the greatest visibility evident near the closed (piston) end. Observations were made in which such suspended particles did not change location significantly for several minutes, even within a foot of the open end. Small external disturbances, such as would be caused by a person walking about near the combustor or the opening of a door, were sufficient to [illegible] the disturbance of equilibrium of the particles [illegible] in the combustor such that a slight [illegible] motion [illegible].

a nearby open window was sometimes sufficient to cause continuous disturbances such that only the particles near the closed end remained relatively unaffected.

The magnitude of the dust particle paths (Figures 22 and 23) observed was seen to be much greater near the open end than near the closed (piston) end. For a given location, the magnitude of the particle paths observed was seen to increase with increase of piston stroke. Some visual estimations of dust particle path length were recorded (Table XII) and plotted in Figure 31. It is difficult to make such estimations accurately and these results must be regarded with caution.

Detailed observations of the dust figures were made in the hope that their behavior, although apparently an incidental phenomenon, might shed additional light on the fundamental nature of the acoustic jet. Figure 24 is a close-up photograph of one of these lateral fines which, unfortunately, does not reveal the significant detail, [illegible] the observable fact that this ridge is made up of tiny particles describing [illegible], with lines parallel to the axis. Incidentally, when looking at the dust figure against the light, it [illegible] central plane. The spacing of the dust figures is somewhat regular (Figure 30), but irregularities are usually present. The distri-

tion of dust figures was observed as a sort of sudden growth from a lateral dust ridge at the bottom of the tube. There were usually several of these dust ridges between dust figures. When a board was clamped over the open end of the resonator, thus closing it, the dust figures all collapsed into dust ridges. They collapsed also if a large wire screen were placed over the middle of the resonator allowing the pressure to escape. Dust figures were occasionally observed to collapse during operation, as a sort of reversal of the growth process. The width of dust figures one foot inside the resonator open end was observed to be about one and one-half inches which is, significantly, about twice the observed particle path length observed at the same location. This observation was for a particle diameter of 0.00[illegible] inches. The same relation between dust figure width and particle path length was observed to exist wherever dust figures were formed.

The rate of longitudinal movement was greatest near the open end. Observations, taken with a 0.0[illegible] inch [illegible] [illegible], showed the average rate near the open end (station 100) to be about three-tenths foot per second; the average rate at one-third the tube length from the open end was two-tenths foot per second; and the movement at two-thirds the tube length from the open end was negligible, although it appeared that the normal

condition was stationary. Dust particles, arriving at the open end of the resonator, [illegible] vortex again, and feed out the central jet. This produces an excellent means of visualizing the low piston stroke flow pattern of the jet as shown in Figures 21, 22, and 23, and shows the degree of symmetry in the flow.

Limitation of Results

The main factor affecting the results obtained was the instrumentation detail with reference to the diameter and length of all tubes and constrictions used in the pressure measurement system. Quantitative evaluation of the data would depend on detailed calculation of the system losses along the lines presented in the discussion of related theory (Refs. 11, 11, 16).

It was found that a basic requirement was the exercise of extreme care with regard to the uniformity of the test equipment at each station. During the course of the investigation, some experimental errors were discovered.

Good reproducibility of results was experienced. The results did not appear to be sensitive to the small variation

in ambient conditions experimented.

The basic assumptions involved in the transfer investigations were that the flow was axially symmetrical, and that the main components of flow were parallel to the axis. These seem justified by a reasonable regularity of the flow visualization results, and the [illegible], [illegible] investigations. The latter appears generally valid except in the area in the [illegible] and between the [illegible] and the jet. [illegible] this region, it appears somewhat valid along the axis of symmetry.

The general conclusions reached through the flow visualization investigations are believed to be valid, although not fully supported by photographs. Part of the phenomenon was verified with the [illegible] with the pressure distribution. The observations of the dust particle path lengths and [illegible] typical [illegible] must be regarded as qualitative, involving [illegible] of small linear dimensions. Also, the dust particle lengths were a function of the dust particle mass.

CONCLUSIONS

These conclusions relate mainly to a single resonator and pulsator configuration and are not intended as absolute generalizations.

(1) It is possible to produce a significant mean-streaming movement in the axial and lateral directions, in a resonator closed at one end and containing air, by generating pulsations at the closed end.

(2) The longitudinal mean pressure gradient has its maximum value near the theoretical resonant frequency of the resonator with corrections for end effects.

(3) The mean pressure distribution and overall flow pattern has axial symmetry in the region sampled.

(4) The longitudinal mean pressure gradient increases with amplitude of pulsator vibration such that pressure values near the closed end increase positively and values near the open end increase negatively.

(5) The rate of change of mean static pressure, with amplitude of pulsator vibration, is greatest near the closed end; least near the open end; and is essentially linear for any

given position along the resonator wall.

(6) The lateral mean static pressure gradient over the major portion of the resonator, is such that the greatest pressures occur near the wall. This gradient approaches zero near the closed end and [illegible] near the open end. [illegible] lateral [illegible] at the open end [illegible] the influence of the strong secondary vortex.

(7) The greatest values of mean velocity along the axis, as indicated by mean static and total pressure measurements, occur at, or just inside, the resonator open end.

(8) The primary aspect of the air movement inside the major portion of the resonator appears to be a longitudinal oscillation in the direction paralleling the axis of symmetry. There appears to be [illegible] periodic wave length such that the largest amplitudes of particle vibration occur near the [illegible] and increased amplitudes of particle vibration occur with [illegible] of [illegible] velocity.

(9) Near the resonant frequency, there is a [illegible], vortex motion of air centered on the open-end edge of the resonator which appears to alternate with a [illegible],

line of [illegible] [illegible] [illegible]. This appears to [illegible] an external-circulation effect [illegible] [illegible] the open end [illegible] conditions [illegible] the vibrating gas column inside the resonator. In cross-section, it appears as an axially symmetrical, relatively shallow, U-shaped, [illegible] [illegible] acting [illegible] [illegible] the source of a jet effect. The apparent depth, to which the [illegible] [illegible] penetrates the resonator, increases with amplitude of pulsator vibration, but remains relatively shallow.

(10) With increased amplitude of pulsator vibration, the vibrating gas column [illegible] [illegible] [illegible] becomes increasingly turbulent.

BIBLIOGRAPHY

1. [illegible], [illegible]: "First Interim Report on the Investigation of Intermittent Flow," Report No. [illegible]; United Aircraft Corporation, East Hartford, Conn., [illegible] September, [illegible].

2. [illegible], [illegible]: "Relation Between Acoustic Phenomena and Dynamic Thrust," Master of Science Thesis, Aeronautical Engineering, University of Minnesota, August 1950.

3. Logan, Joseph G., Jr.: "Suggested Forms of Air Duct Motors Utilizing Intermittent Combustion," Parts I and II, Project Squid, Tech. Memo. No. CAL-17, Cornell Aeronautical Laboratory, Inc., Buffalo 21, New York, 28 February, 1948.

4. Rudinger, George and Rinaldi, [illegible]: "The Construction of Wave Diagrams for the Study of One-Dimensional Non-Steady Gas Flow," Technical Memorandum No. CAL-24, Project Squid, Cornell Aeronautical Laboratory, Inc., Buffalo 21, New York, 10 March, 1949.

5. Rudinger, G., Logan, J., and [illegible]: "Investigations of Acoustic Jets," (a) Part I, Report No. CAL-15, (b) Part II, Report No. CAL-15; Project Squid, Cornell Aeronautical Laboratory, Inc., Buffalo 21, New York, 10 March, 1948.

6. Rayleigh, John W. S.: "The Theory of Sound," Vol. I, Dover Publications, New York, 1945.

7. Morse, Philip M.: "Vibration and Sound," McGraw Hill Book Co., Inc., 1936.

8. Ingard, U.: "On the Radiation of Sound into a Circular Tube, with an Application to Resonators," Acta Polytech. 28 (Elect. Eng. Ser. 1, No. 5) Trans. Chalmers Univ. Tech. Gothenburg 70, 3-[illegible] (1948). In English. The case of a plane piston source in rigid tube is treated theoretically.

9. Wood, A. B.: "Textbook of Sound," G. Bell and Sons, Ltd., 1930.

10. Liston, J.: "Aircraft Engine Design," McGraw-Hill Book Co., New York, 1942.

11. Iberall, A. S.: "Attenuation of Oscillatory Pressures in Instrument Lines," Transactions of the ASME, Vol. 72, No. 5; July, 1950.

12. Taback, Israel: "The Response of Pressure Measuring Systems to Oscillating Pressures," NACA TN 1819, February, 1949.

13. [illegible], J.: Physical Review, [illegible], [illegible], 194[illegible].

14. Pope, Alan: "Wind-Tunnel Testing," John Wiley and Sons, Inc., New York, 1952.

15. Liepmann, H. W., Puckett, A. E.: "Aerodynamics of a Compressible Fluid," John Wiley and Sons, Inc., New York, 1947.

16. Wildhack, W. A.: "Pressure Drop in Tubing in Aircraft Instrument Installations," NACA TN 593, Wash., February, 1937.

TABLE I

DETERMINATION OF RESONANT FREQUENCY FOR BASIC

RESONATOR CONFIGURATIONS*

(Resonator Wall Mean Static Pressure Data)

Instrumentation: **Wall Static   Piston Stroke: [illegible] in.
End Edge Shape: Square   Resonator Length: 107.[illegible] in.

Sta. No.			6	10
X (in. from open end)			[illegible]	102
RPM	H_a	t	h_s	h_s
1954	29.24	[illegible]	-1.62	[illegible]
1958	29.24	[illegible]	-1.91	[illegible]
1967	29.24	[illegible]	-2.01	5.77
1974	29.24	[illegible]	-2.04	[illegible]
1979	29.24	85		6.15
1984	29.24	[illegible]	-2.12	6.15
1992	29.24	[illegible]	-2.17	[illegible]
[illegible]	29.24	[illegible]		6.36
1901	29.24	[illegible]	-2.11	[illegible]
1905	29.24	[illegible]		[illegible]
1911	29.24	[illegible]		[illegible].45
1914	29.24	[illegible]	[illegible]	6.21
1916	29.24	[illegible]	-2.05	[illegible]
[illegible]	29.24	[illegible]		5.95
1940	29.24	[illegible]	-1.[illegible]	[illegible]
1961	29.24	[illegible]	-1.[illegible]	[illegible]
1970	29.24	[illegible]	-1.[illegible]	[illegible]

*See Apparatus and Nomenclature

**See Limitations

TABLE II

[illegible]

[illegible] CONFIGURATION**

([illegible] Wall [illegible] Static Pressure Data)

Instrumentation: Wall Static   Piston Stroke: [illegible] in.

Sta. No.	14	18
x	0	[illegible]
H_a	[illegible]	[illegible]
t	[illegible]	[illegible]
L	[illegible]	102.4
End Edge Shape	Sharp	Sharp
RPM	h_s	h_s
1795	-2.25	[illegible]
1800	[illegible]	[illegible]
1808	-2.51	[illegible]
1813	-2.87	[illegible]
1820	-2.87	[illegible]
1828	-2.87	[illegible]
1836	[illegible]	4.10
1843	-3.10	[illegible]
1852	-3.21	[illegible]
1860	[illegible]	4.40
1864	-2.95	[illegible]
1867	-3.02	[illegible]
1875	[illegible]	[illegible]
1884	[illegible]	[illegible]
1893	-2.56	[illegible]
1904	-2.52	[illegible]
1908	-2.45	[illegible]
1917	-2.25	[illegible]

*See Apparatus and Nomenclature

**See Limitations

TABLE III

VARIATION OF RESONATOR WALL MEAN STATIC PRESSURE WITH FREQUENCY

Instrumentation: Small Station Piston Stroke: [illegible] in.
End Edge Shape: Square Resonator Length: 107.[illegible] in.
Resonator: Basic Configuration

RPM		1948	1970	[illegible]	[illegible]	1916	[illegible]	[illegible]	[illegible]
H_a		[illegible]	[illegible]	[illegible]	29.24	[illegible]	29.22	29.24	29.24
t		80	[illegible]	[illegible]	[illegible]	[illegible]	[illegible]	[illegible]	80
Sta. No.	x	h_s	h_s	h_s	h_s	h_s	h_s	h_s	h_s***
1	0	-2.46	-3.08	-3.27	[illegible]	-5.42	-3.20	[illegible]	[illegible]
2	6	-1.76	-2.27	-2.41	-2.55	[illegible]	-2.25	[illegible]	[illegible]
3	12	-1.78	-2.21	[illegible]	[illegible]	-2.21	-2.31	[illegible]	-2.18
4	18	-1.58	[illegible]	[illegible]	-2.13	[illegible]	-1.93	-1.73	[illegible]
5	24	-1.32	-1.52	-1.43	[illegible]	-1.14	[illegible]	[illegible]	[illegible]
6	30	-1.63	[illegible]	[illegible]	-2.02	-2.08	[illegible]	-1.72	[illegible]
7	36	[illegible]	[illegible]	[illegible]	[illegible]	[illegible]	[illegible]	-1.28	
8	42	-0.17	-0.18	[illegible]	[illegible]	[illegible]	[illegible]	[illegible]	[illegible]
9	48	+0.14	[illegible]	[illegible]	[illegible]	0.00	+0.02	[illegible]	
10	54	1.07	+1.11	1.19	1.08	+0.97	[illegible]	+0.91	
11	60	1.90	[illegible]	[illegible]	[illegible]	2.17	[illegible]	[illegible]	[illegible]
12	66	[illegible]	[illegible]	[illegible]	[illegible]	[illegible]	[illegible]	[illegible]	
13	[illegible]	[illegible]	[illegible]	[illegible]	[illegible]	[illegible]	[illegible]	[illegible]	[illegible]
14	[illegible]	[illegible]	[illegible]	[illegible]	[illegible]	[illegible]	[illegible]	[illegible]	
15	[illegible]	[illegible]	[illegible]	[illegible]	[illegible]	[illegible]	[illegible]	[illegible]	[illegible]
16	[illegible]	[illegible]	[illegible]	[illegible]	[illegible]	[illegible]	[illegible]	[illegible]	[illegible]
17	[illegible]	[illegible]	[illegible]	[illegible]	[illegible]	[illegible]	[illegible]	[illegible]	
18	102	[illegible]	[illegible]	[illegible]	[illegible]	[illegible]	[illegible]	[illegible]	[illegible]

*See Apparatus and Nomenclature

**See Limitations

***Modified connection (small tube) at station number [illegible]
(See Figure [illegible])

TABLE IV

RESONATOR WALL MEAN STATIC PRESSURE DATA,

SHOWING EFFECT OF END CAP SHAPE*

Instrumentation: Small Static Modified
Piston Stroke: 0.878 in.
Resonator Length: 100.4 in.
Resonator: Basic configuration plus modified [illegible]

End Edge Shape		Sharp	Sharp	Square
P_a		29.27	29.59	29.31
t		86	86	85
RPM		1961	1801	1801
Sta. No.	x	h_s	h_s	h_s
1a	0	-6.00	-2.10	-2.94
1	3	-3.00		-2.78
2	8	-2.51		-2.33
3	14	-2.11		-1.87
4	20	-3.12	-2.17	-2.05
5	26	-1.76		-1.47
6	32	-2.12	-2.10	-2.04
7	[illegible]	-1.08		-1.[illegible]
8	44	-0.82		-0.[illegible]
9	50	-0.57	-0.02	-0.12
10	56	+0.42		+1.11
11	62	1.00		2.03
12	68	1.80	+1.90	2.81
13	74	2.60		3.50
14	80	2.13		3.87
15	86	3.11	1.37	1.63
16	92	2.50		3.40
17	98	1.90		7.20
18	104	+1.22	+1.82	+2.51

*See Apparatus and Nomenclature

**See Limitations

TABLE V

RESONATOR WALL MEAN STATIC PRESSURE SURVEY

WITH VARIABLE PISTON STROKE**

Instrumentation: Wall Static   Resonator: *Basic Configuration
End Edge Shape: Square   Resonator Length: 107.4 in.

Piston Stroke, in.		0.051	0.292	0.5[illegible]	0.722	0.970
RPM		1303	1303	1302	1303	1302
H_a		29.42	29.42	29.42	29.42	29.42
t		83	83	83	83	83
Sta. No.	x	h_s	h_s	h_s	h_s	h_s
1	0	-0.13	-0.35	-2.0[illegible]	-2.71	-2.31
2	6	-0.09	-0.50	-1.10	-1.69	-2.15
3	12	-0.03	-0.57	-1.30	-1.75	-2.31
4	18	-0.02	-0.74	-1.19	-1.71	-2.20
5	24	+0.03	-0.72	-0.91	-1.18	-1.66
6	30	-0.03	-0.57	-1.27	-1.33	-2.13
7	36	-0.03	-0.70	-0.98	-1.51	-1.53
8	42	+0.03	-0.11	-0.36	-0.73	-0.33
9	48	0.07	+0.03	+0.08	+0.03	+0.02
10	54	0.12	0.35	0.63	0.73	0.9[illegible]
11	60	0.19	0.65	1.03	1.34	1.62
12	66	0.22	0.90	1.33	1.60	2.10
13	72	0.21	1.00	1.30	2.32	3.20
14	78	0.20	1.31	2.08	3.29	[illegible]
15	84	0.22	1.40	2.72	3.70	[illegible]
16	90	0.19	1.03	3.11	3.21	[illegible]
17	96	0.[illegible]	1.71	3.72	3.21	3.21
18	102	+0.32	+1.11	+2.71	+3.12	+4.03

*See Apparatus and Nomenclature

**See Limitations

TABLE VI

CALCULATED THRUST VALUES

(Pressure Data from Figure [illegible] and Table [illegible])

t	V_a	h_g (at piston)	h_g (at [illegible])	T (lbs)
[illegible]	[illegible]	[illegible]	[illegible]	[illegible]
[illegible]	[illegible]	[illegible]	[illegible]	[illegible]
[illegible]	[illegible]	[illegible]	[illegible]	[illegible]
[illegible]	[illegible]	[illegible]	[illegible]	[illegible]
[illegible]	[illegible]	[illegible]	-0.1	[illegible]

TABLE VII

[illegible]

Instrumentation: [illegible] (Probe 2) Piston Stroke: 0.??? in. [illegible] Square
[illegible] configuration Connecting length: 107.9 cm.

Run No.	[illegible]	[illegible]	[illegible]	[illegible]	7	7	7	7	12	12	14	14	17	17	17	17
[illegible]	1001	1001	1002	1002	1002	1002	1002	1002	1002	1002	1001	1001	1001	1001	1002	1002
[illegible]	[illegible].17	[illegible]	[illegible]	[illegible]	[illegible]	[illegible]	[illegible]	[illegible]	[illegible]	[illegible]	[illegible]	[illegible]	[illegible]	[illegible]	[illegible]	[illegible]
[illegible]	84	84	84	84	84	84	84	84	84	84	84	84	85	85	85	85
φ***	0°	180°	90°	270°	0°	180°	90°	270°	0°	180°	90°	270°	0°	180°	90°	270°
r	[illegible]	[illegible]	[illegible]	[illegible]	[illegible]	[illegible]	[illegible]	[illegible]	[illegible]	[illegible]	[illegible]	[illegible]	[illegible]	[illegible]	[illegible]	[illegible]
0	-1.50		-1.52		+0.14		+0.13		+6.01		+5.5[illegible]		[illegible].10	+5.21	+6.10	+6.0[illegible]
0.25	[illegible]	[illegible]	[illegible]	-4.02	[illegible]	-1.42	[illegible]	-1.45	7.00	[illegible]	[illegible]	[illegible]	[illegible]	[illegible]	[illegible]	[illegible]
0.75	[illegible]	-4.20	-4.00	-1.28	-1.74	-1.44	[illegible]	[illegible]	[illegible]	[illegible]	[illegible]	[illegible]	[illegible]	[illegible]	[illegible]	[illegible]
1.25	[illegible]	-1.20							[illegible]	[illegible]			[illegible]	[illegible]		
1.75	-4.20	[illegible]	[illegible]	[illegible]	[illegible]	[illegible]	[illegible]	[illegible]	[illegible]	[illegible]	[illegible]	[illegible]	[illegible]	[illegible]	[illegible]	[illegible]
2.25	[illegible]	[illegible]							[illegible]	[illegible]			[illegible]	[illegible]	[illegible]	[illegible]
2.75	[illegible]	[illegible]	[illegible]	[illegible]	[illegible]	[illegible]	[illegible]	[illegible]	[illegible]	7.17	[illegible]	[illegible]	[illegible]	[illegible]	[illegible]	[illegible]
[illegible]	[illegible]	[illegible]							[illegible]	[illegible]			[illegible]	[illegible]	[illegible]	[illegible]
1.75	[illegible]	[illegible]	[illegible]	[illegible]	[illegible]	[illegible]	[illegible]	[illegible]	[illegible]	[illegible]	[illegible]	[illegible]	[illegible]	[illegible]	[illegible]	[illegible]
1.25	[illegible]	[illegible]							[illegible]	[illegible]			[illegible]	[illegible]		
0.75	[illegible]	[illegible]	[illegible]	[illegible]	[illegible]	[illegible]	[illegible]	[illegible]	[illegible]	[illegible]	[illegible]	[illegible]	[illegible]	[illegible]	[illegible]	[illegible]
0.25	[illegible]	[illegible]	[illegible]	[illegible]	[illegible]	-0.97	[illegible]	[illegible]	[illegible]	[illegible]	[illegible]	[illegible]	[illegible]	[illegible]	[illegible]	[illegible]
0		[illegible]		-1.7[illegible]		+0.0[illegible]		+0.12		+5.9[illegible]		[illegible]		[illegible].10		+5.0[illegible]

[illegible]
[illegible]
[illegible] position of probe [illegible]

TABLE VIII

ONE-WAY, INTERNAL RADIAL TRAVERSE, MEAN STATIC PRESSURE DATA**

Instrumentation: *Internal Traverse (Probe 2)
Resonator: *Basic configuration
Resonator length: 107.4 in.

Piston Stroke: 0.978 in.
End Edge Shape: Square

Sta. No.	1	[illegible]	4	5	6	[illegible]	9	10	11	13	14	15	16	18
RPM	1900	1902	1900	1901	1902	1902	1902	1900	1902	1902	1902	1901	1901	1902
U_a	29.03	[illegible]	[illegible]	29.0[illegible]	29.03	29.2[illegible]	29.26	29.03	29.26	29.2[illegible]	29.[illegible]	29.06	29.0[illegible]	29.2[illegible]
t	85	[illegible]	85	85	85	83	82	85	82	82	82	[illegible]	85	82
ϕ***	0°	0°	0°	0°	0°	0°	0°	0°	0°	0°	0°	0°	0°	0°
r^1	h_s	h_s	h_s	h_s	h_s	h_s	h_s	h_s	h_s	h_s	h_s	h_s	h_s	h_s
0	-1.[illegible]	-1.7[illegible]	-1.[illegible]	-0.7[illegible]	-0.11	+0.[illegible]	+1.[illegible]	+1.[illegible]	+2.77	+3.77	+4.20	+4.27	+5.32	+5.75
0.25	-5.92		-2.5[illegible]	-2.25	-1.22			1.16				4.20	5.29	
0.75	-[illegible].92		-7.25	-2.[illegible]	-2.15			1.0[illegible]				1.75	5.24	
1.25	-4.52													
1.75	-7.00		-3.26	-2.05	-2.15			1.12				4.71	5.26	
2.25														
2.75	-[illegible]	-[illegible]	-3.2[illegible]	-2.[illegible]	-2.17	-0.76	+0.12	1.14	+1.77	+3.35	+4.1[illegible]	[illegible]	[illegible].24	+5.75
3.25														
1.75	-[illegible]		-3.2[illegible]	-2.92	-2.1[illegible]			1.1[illegible]				[illegible].92	5.22	
1.25	-[illegible]													
0.75	-4.2[illegible]		-3.29	-3.00	-2.10			1.12				[illegible].20	5.15	
0.25	-5.72		-3.2[illegible]	-3.0[illegible]	-2.13			+1.0[illegible]				+4.20	+5.10	
0														

*See Apparatus and Notation.
**Typed limitations.
***Refers to roll position of probe introduction. See Nomenclature.

TABLE [illegible]

[illegible], INTERNAL AXIAL TRAVERSE, [illegible] TOTAL PRESSURE DATA*

Instrumentation: *Internal Traverse. Piston Stroke: 0.[illegible] in.
Resonator: *Basic Configuration. [illegible] Edge Shape: Square
Resonator Length: 107.[illegible] in.

Std. No.	2	3	15	19	17
RPM	1992	1992	1992	1997	1992
V_a	23.47	29.02	[illegible]	27.26	[illegible]
[illegible]	[illegible]	35	35	32	[illegible]
ϕ***	[illegible]	0°	50	0°	0°
Type of Probe	L-head-3	L-head-3	L-head-[illegible]	Cyl.-4	L-head-[illegible]

Probe Opening Facing Toward Piston:

r^1	h_o	h_o	h_o	h_o	h_o
0.25	-0.2[illegible]	-0.2[illegible]	+0.17	+2.4[illegible]	+3.27
0.75	-0.41	-0.4[illegible]	0.15	2.45	3.3[illegible]
1.75	-0.48	-0.4[illegible]	0.1[illegible]	2.48	3.40
2.75	-0.5[illegible]	-0.5[illegible]	0.17	2.40	3.40
1.75	-0.44	-0.4[illegible]	+0.1[illegible]	+2.41	+3.40

Probe Opening Facing Away from Piston:

r^1	h_o	h_o	h_o	h_o	h_o
0.25	-0.[illegible]	-0.92	+2.59	+2.40	+3.27
0.75	-0.5[illegible]	-0.[illegible]	2.[illegible]	2.4[illegible]	3.27
1.75	-0.34	-0.3[illegible]	2.[illegible]	2.3[illegible]	3.2[illegible]
2.75	-0.40	-0.41	2.60	2.3[illegible]	3.23
1.75	-0.[illegible]	-0.73	+2.65	+2.34	+3.28

*See Apparatus and Nomenclature.

**See Limitations.

***Refers to wall position of probe introduction. See Nomenclature.

TABLE [illegible]

[illegible] TOTAL PRESSURE SURVEY [illegible]

Instrumentation: *Internal traverse, cylinder probe (1)
Resonator: *Basic configuration   Piston stroke: [illegible] in.
Resonator Length: 1[illegible]7.4 in.   End Edge Shape: Square

Distance from tube wall, in. (r^1)		2.75	2.75
[illegible]		[illegible]	[illegible]
[illegible]		[illegible]	[illegible]
ϕ***		[illegible]	[illegible]
Probe Opening Orientation		Facing Piston	Away from Piston
Stn. No.	RPM	[illegible]	[illegible]
1	1902	-1.41	-0.67
2	1902	-1.30	-0.38
3	1901	-0.82	-0.57
4	1900	-0.56	-0.62
5	1903	-0.75	-0.46
6	1900	+0.00	-0.20
7	1903	0.62	+0.79
8	1907	1.11	0.97
9	1905	1.[illegible]0	1.74
10	1807	2.50	2.40
11	1902	3.10	3.75
12	1901	3.60	3.50
13	1902	4.35	4.75
14	1902	5.10	5.10
15	1903	5.55	5.71
16	1902	5.90	5.92
17	1902	6.25	6.25
18	1901	6.15	+6.15

*See Apparatus and Nomenclature.

**See Limitations.

***Refers to wall position of probe introduction. See Nomenclature.

TABLE XIa

LATERAL MEAN PRESSURE DATA**

(Traverse in Horizontal Axial Plane)

Instrumentation: *External traverse Piston stroke: 0.??? in.
Resonator: *Basic configuration Open end edge: Square
Resonator Length: 107.4 in.

pL	0.5	0.5	0.5	2.5	2.5	2.5
RPM	1801	1801	1801	1801	1801	1801
U_a	29.42	29.42	29.42	29.42	29.42	29.42
t	84	84	84	84	84	84
Type of Probe*	(5)	(5)	(6)	(5)	(5)	(6)
φ***	90°	90°	90°	90°	90°	90°
r	h_o(in)"	h_o(out)"	h_s	h_o(in)	h_o(out)	h_s
-4.0	-0.09	-0.26		-0.08	-0.33	
-3.5	-0.24	-0.41	-0.59			
-3.0	-1.05	-0.45	-0.97	+0.30	-0.40	-0.90
-2.5	-1.30	-0.64	-2.28			
-2.0	-0.53	-0.41	-2.13	0.71	-0.21	-0.39
-1.5	-0.13	-0.31	-1.70			
-1.0	-0.70	-0.25	-1.97	0.73	-0.12	-0.50
-0.5	-0.90	-0.39	-1.90			
0.0	-0.34	-0.13	-1.95	0.27	-0.12	-0.60
+0.5	-0.23	-0.20	-1.84			
1.0	-0.37	-0.34	-2.77	0.95	-0.29	-0.90
1.5	-0.47	-0.41	-2.50			
2.0	-0.71	[illegible]	-2.93	1.1[illegible]	-0.50	-1.19
2.5			-2.43			
3.0	-0.59	-0.75	-0.89	+0.75	-0.46	-0.72
3.5			-0.19			
4.0			-0.14			
5.0			-0.03	-0.09	-0.14	-0.14
6.0			-0.08			-0.05
7.0						-0.02

*See Apparatus and Nomenclature.
**See Limitations.
***Refers to wall position or direction of probe introduction, "r" is positive to side from which probe is introduced. See Nomenclature.
"Total head opening faces towards the piston (in) or away from the piston (out).

TABLE [illegible]

[illegible]

([illegible])

[illegible] [illegible]
[illegible] [illegible]
[illegible] Length. 107.4 in.

Run		1901	1901	1901
[illegible]		[illegible].42	[illegible].42	[illegible].42
[illegible]		[illegible]	[illegible]	[illegible]
[illegible]		([illegible])	([illegible])	([illegible])
[illegible]		[illegible]	[illegible]	[illegible]
r	[illegible]	h_0(in)	h_0(out)	[illegible]
-4.0	0	+0.76	-0.47	-0.5[illegible]
-3.0	0	0.[illegible]	-0.[illegible]	-0.[illegible]
-2.0	0	0.61	-0.15	-0.[illegible]
-1.0	0	0.7[illegible]	-0.[illegible]	-0.[illegible]
0.0	0	[illegible]	-0.11	-0.[illegible]
+1.0	0	[illegible]	-0.16	-0.[illegible]
[illegible].0	0	[illegible]	-0.[illegible]	-0.[illegible]
[illegible].0	[illegible]	[illegible]	-0.[illegible]	-0.[illegible]
[illegible].0	0	[illegible]	-0.4[illegible]	-0.[illegible]
[illegible].0	0	+0.10	[illegible]	-0.[illegible]
[illegible].0	[illegible]	-0.1[illegible]	-0.1[illegible]	-0.[illegible]
0.0	12	+0.[illegible]		-0.[illegible]
0.0	[illegible]	[illegible]		-0.[illegible]
0.0	[illegible]	0.[illegible]		-0.[illegible]
0.0	[illegible]	0.[illegible]		-0.[illegible]
0.0	[illegible]	0.[illegible]		-0.[illegible]
0.0	[illegible]	+0.[illegible]		-0.[illegible]

[illegible]

[illegible]

[illegible] "r" is positive [illegible] introduced. [illegible] [illegible]lature.

[illegible] towards the piston (in) or away from the piston (out).

TABLE XII

[illegible] PENETRATION [illegible] AND PARTICLE PATH

LENGTHS FROM VISUAL OBSERVATIONS AND PHOTOGRAPHS

Piston Stroke, in.	Depth of Observed Penetration, in.	Estimated from
0.094	1.5	Visual Observation
0.094	1.5	Photograph (see Figs. [illegible])
0.2[illegible]	[illegible]	Visual Observation
0.5[illegible]	[illegible]	Visual Observation
0.766	11.0	Photograph (see Figure [illegible])
0.[illegible]	13.0	Visual Observation

Piston Stroke, in.	*Observed Particle Path Length, in.			
	Sta. 3	Sta. 7	Sta. 10	Sta. 14
0.09[illegible]	[illegible]	0.5	0.2	0.1
0.2[illegible]	1.5			0.1
0.5[illegible]	2.5			0.5
0.766	Observation uncertain			
0.[illegible]	Observation uncertain			

*Note: Particle path observations were based on readily visible particles which [illegible] of considerable mass, [illegible] along [illegible] the vibrating particles [illegible] apparent as straight lines. Consequently this data should be regarded as qualitative.

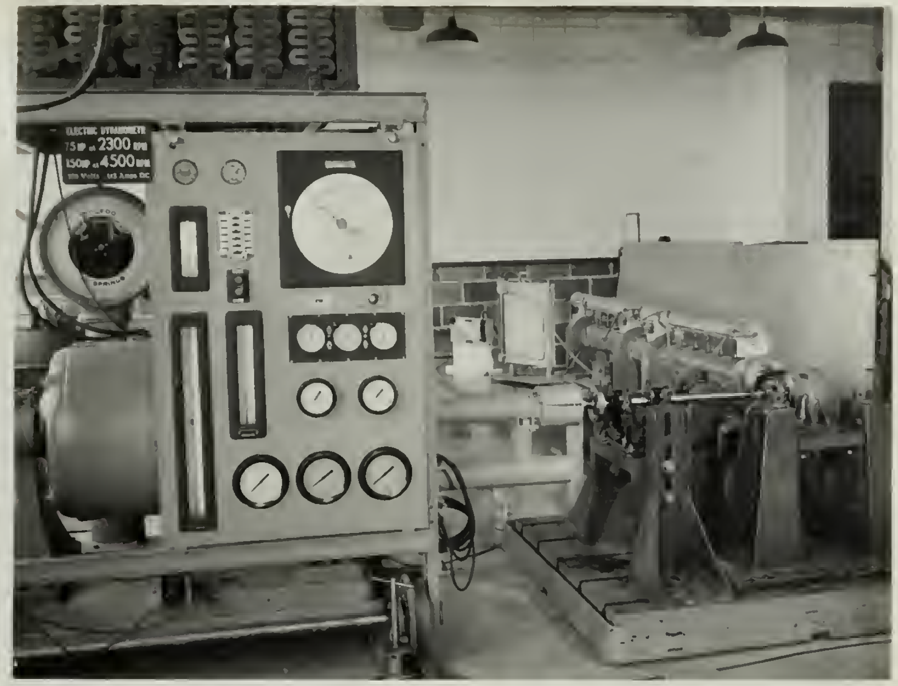
ELECTRIC DYNAMOMETER
75 HP at 2300 RPM
150 HP at 4500 RPM

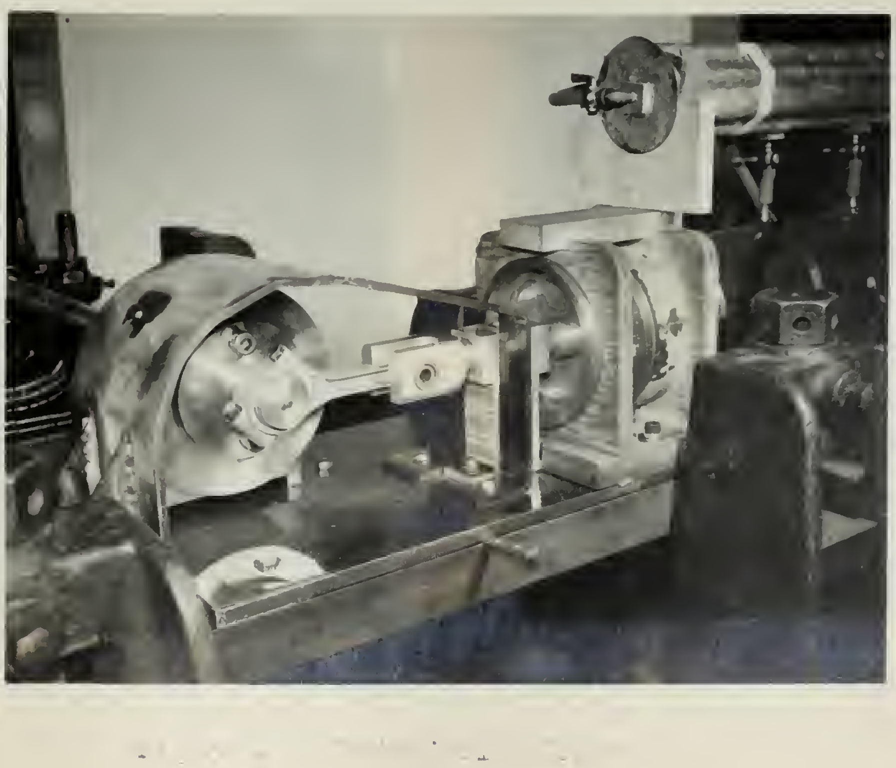

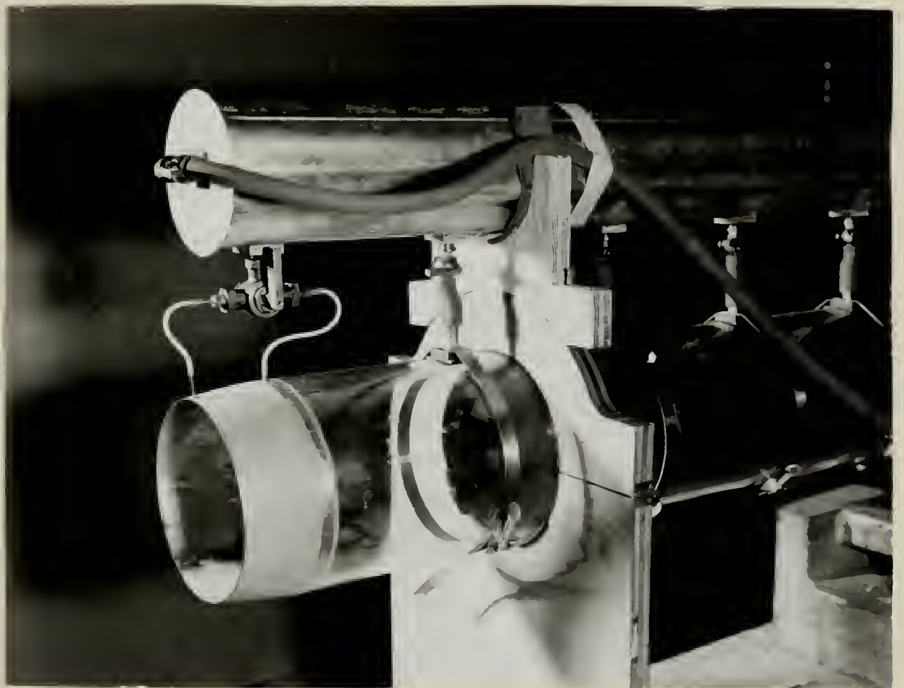

Figure 3 Resonator Open and Modification with "Wall Static" Instrumentation.

Figure 4 External Traverse Arrangement

Figure 5 Internal Traverse Arrangement

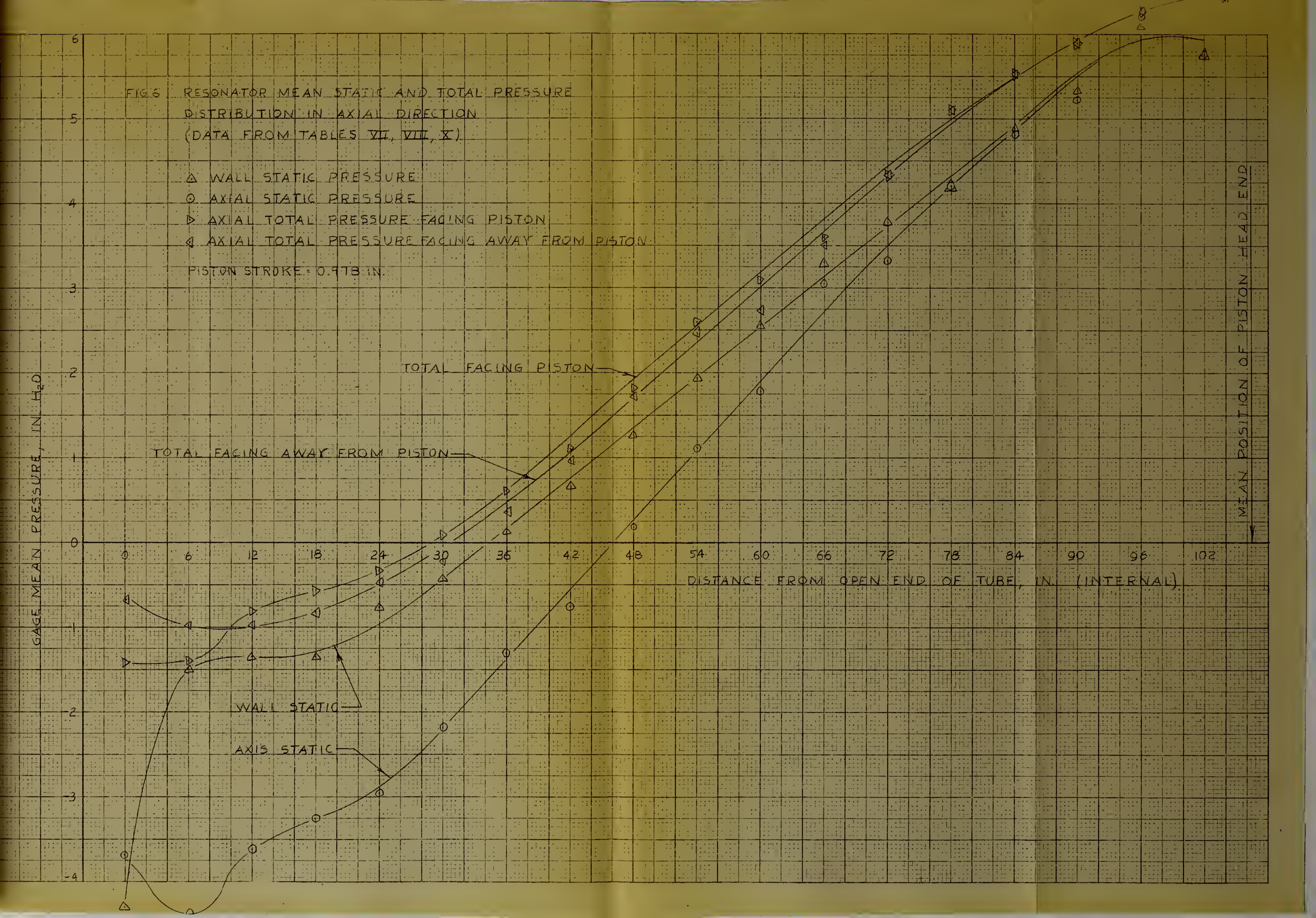
FIG. 6 RESONATOR MEAN STATIC AND TOTAL PRESSURE DISTRIBUTION IN AXIAL DIRECTION
(DATA FROM TABLES VII, VIII, X)
△ WALL STATIC PRESSURE
○ AXIAL STATIC PRESSURE
▷ AXIAL TOTAL PRESSURE FACING PISTON
◁ AXIAL TOTAL PRESSURE FACING AWAY FROM PISTON
PISTON STROKE: 0.978 IN.
TOTAL FACING PISTON
TOTAL FACING AWAY FROM PISTON
WALL STATIC
AXIS STATIC
GAGE MEAN PRESSURE, IN. H_2O
DISTANCE FROM OPEN END OF TUBE, IN. (INTERNAL)
MEAN POSITION OF PISTON HEAD END
6
5
4
3
2
1
0
-1
-2
-3
-4
0
6
12
18
24
30
36
42
48
54
60
66
72
78
84
90
96
102

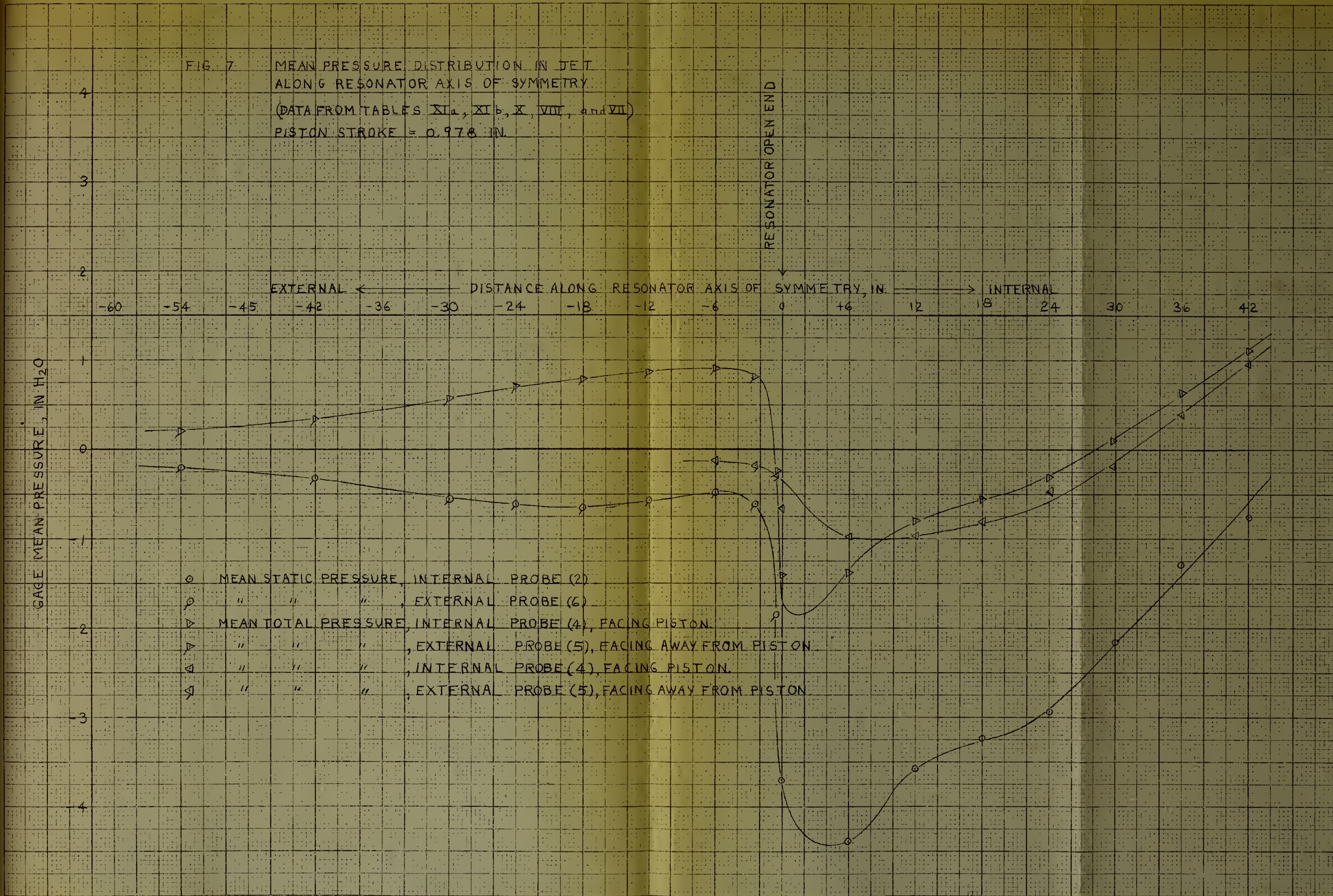

FIG. 7 MEAN PRESSURE DISTRIBUTION IN JET ALONG RESONATOR AXIS OF SYMMETRY
(DATA FROM TABLES XIa, XIb, X, VIII, and VII)
PISTON STROKE = 0.978 IN.
RESONATOR OPEN END
EXTERNAL ← DISTANCE ALONG RESONATOR AXIS OF SYMMETRY, IN. → INTERNAL
-60
-54
-48
-42
-36
-30
-24
-18
-12
-6
0
+6
12
18
24
30
36
42
4
3
2
1
0
-1
-2
-3
-4
GAGE MEAN PRESSURE, IN H_2O
MEAN STATIC PRESSURE, INTERNAL PROBE (2)
" " " , EXTERNAL PROBE (6)
MEAN TOTAL PRESSURE, INTERNAL PROBE (4), FACING PISTON
" " " , EXTERNAL PROBE (5), FACING AWAY FROM PISTON
" " " , INTERNAL PROBE (4), FACING PISTON
" " " , EXTERNAL PROBE (5), FACING AWAY FROM PISTON

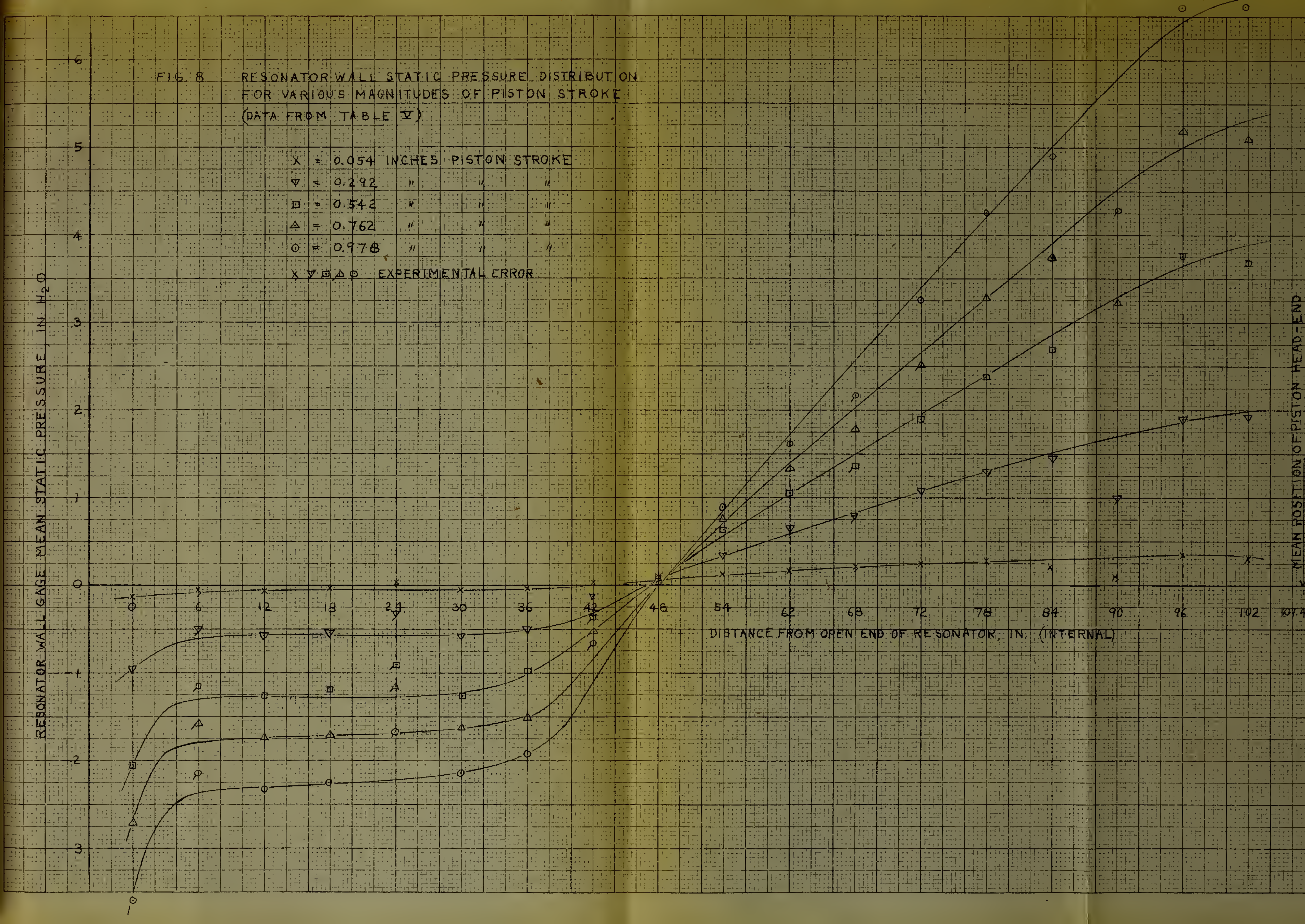

FIG. 8 RESONATOR WALL STATIC PRESSURE DISTRIBUTION FOR VARIOUS MAGNITUDES OF PISTON STROKE
(DATA FROM TABLE V)
X = 0.054 INCHES PISTON STROKE
▽ = 0.292 " " "
⊡ = 0.542 " " "
△ = 0.762 " " "
⊙ = 0.978 " " "
X ▽ ⊡ △ ⊙ EXPERIMENTAL ERROR
RESONATOR WALL GAGE MEAN STATIC PRESSURE, IN. H_2O
DISTANCE FROM OPEN END OF RESONATOR, IN. (INTERNAL)
MEAN POSITION OF PISTON HEAD-END
+6
5
4
3
2
1
0
-1
-2
-3
0
6
12
18
24
30
36
42
48
54
62
68
72
78
84
90
96
102
107.4

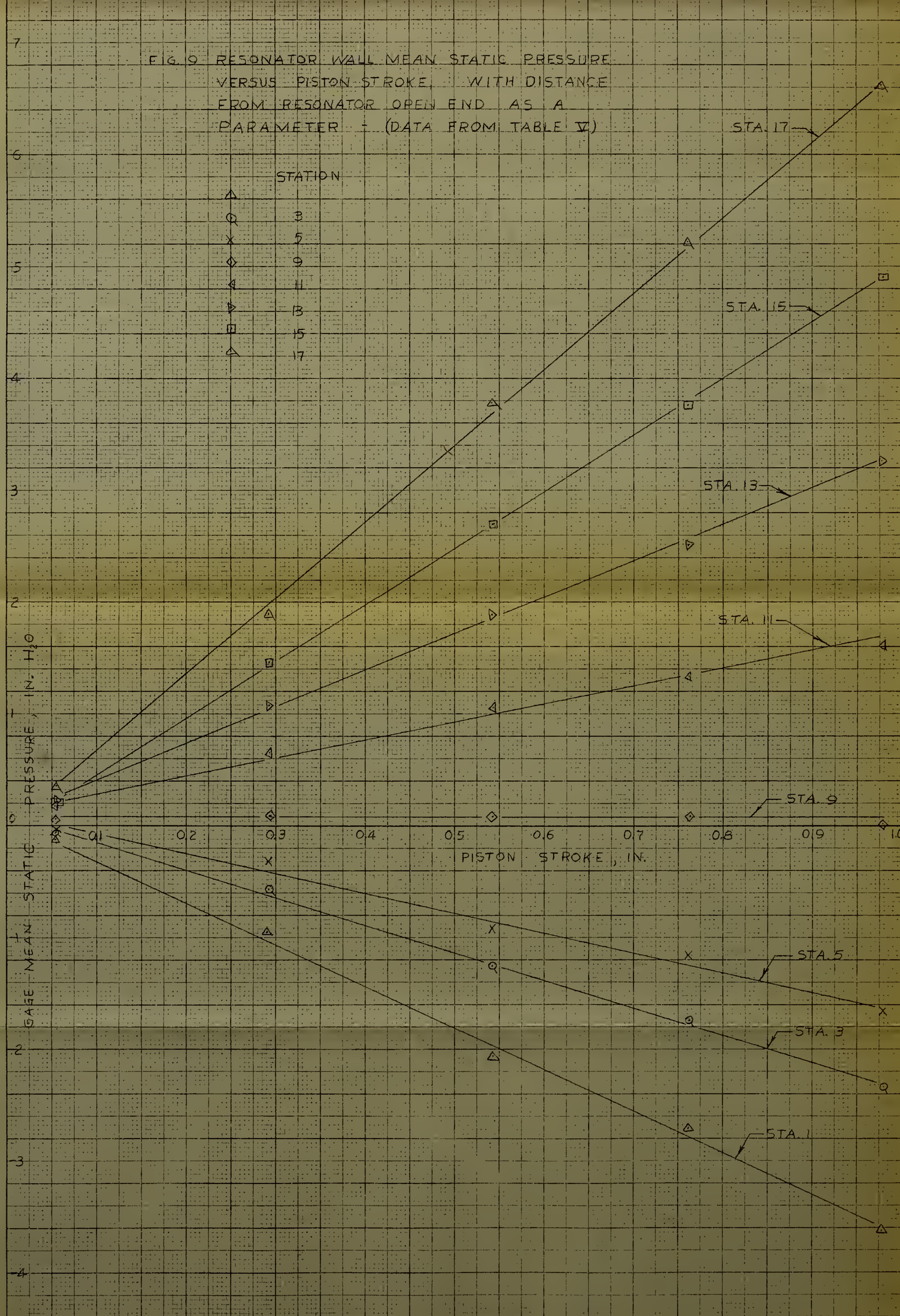
FIG. 9 RESONATOR WALL MEAN STATIC PRESSURE
VERSUS PISTON STROKE, WITH DISTANCE
FROM RESONATOR OPEN END AS A
PARAMETER - (DATA FROM TABLE V)
STATION
3
5
9
11
13
15
17
STA. 17
STA. 15
STA. 13
STA. 11
STA. 9
STA. 5
STA. 3
STA. 1
PISTON STROKE, IN.
GAGE MEAN STATIC PRESSURE, IN. H_2O
7
6
5
4
3
2
1
0
-1
-2
-3
-4
0.1
0.2
0.3
0.4
0.5
0.6
0.7
0.8
0.9
1.0

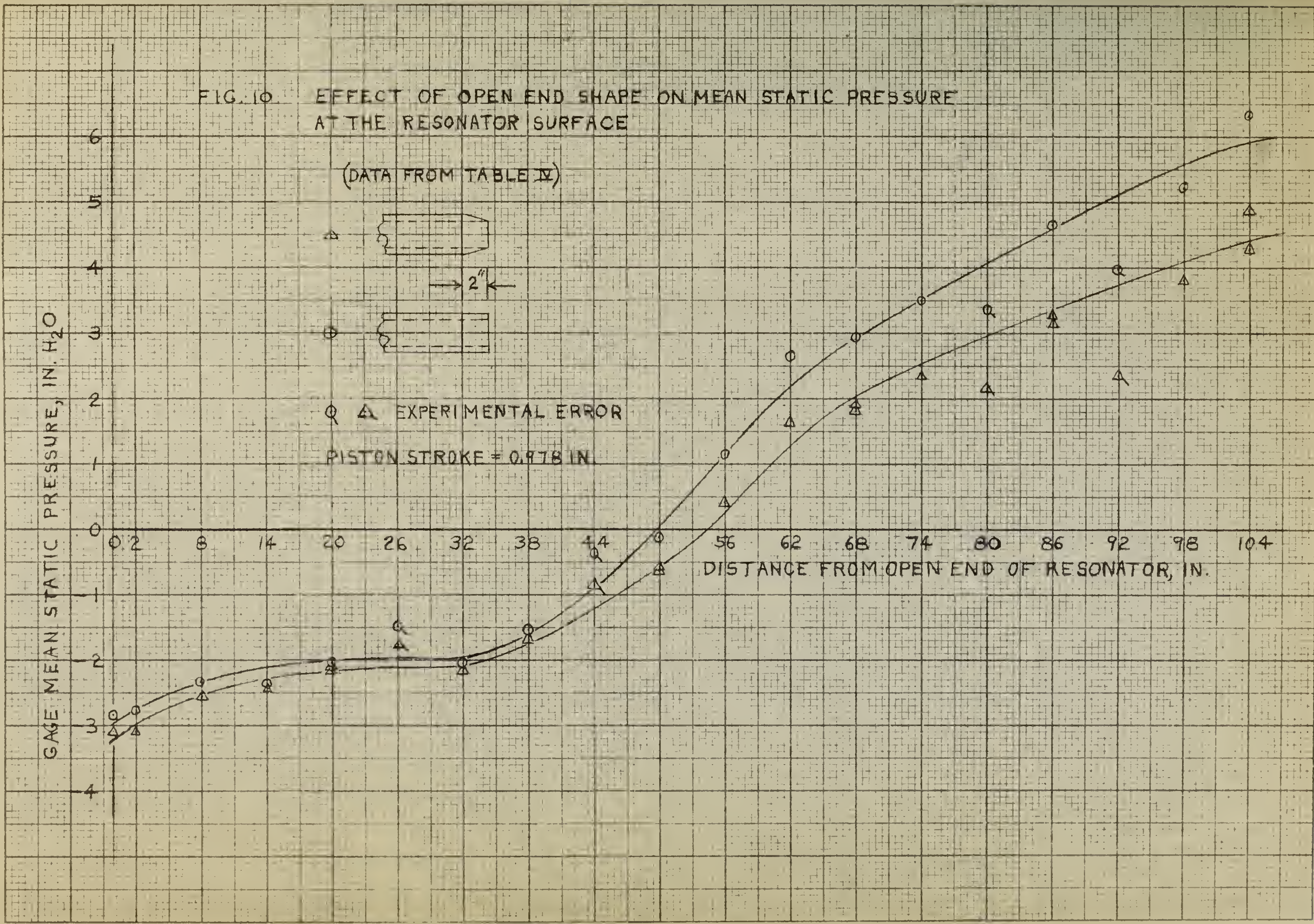

FIG. 10 EFFECT OF OPEN END SHAPE ON MEAN STATIC PRESSURE AT THE RESONATOR SURFACE

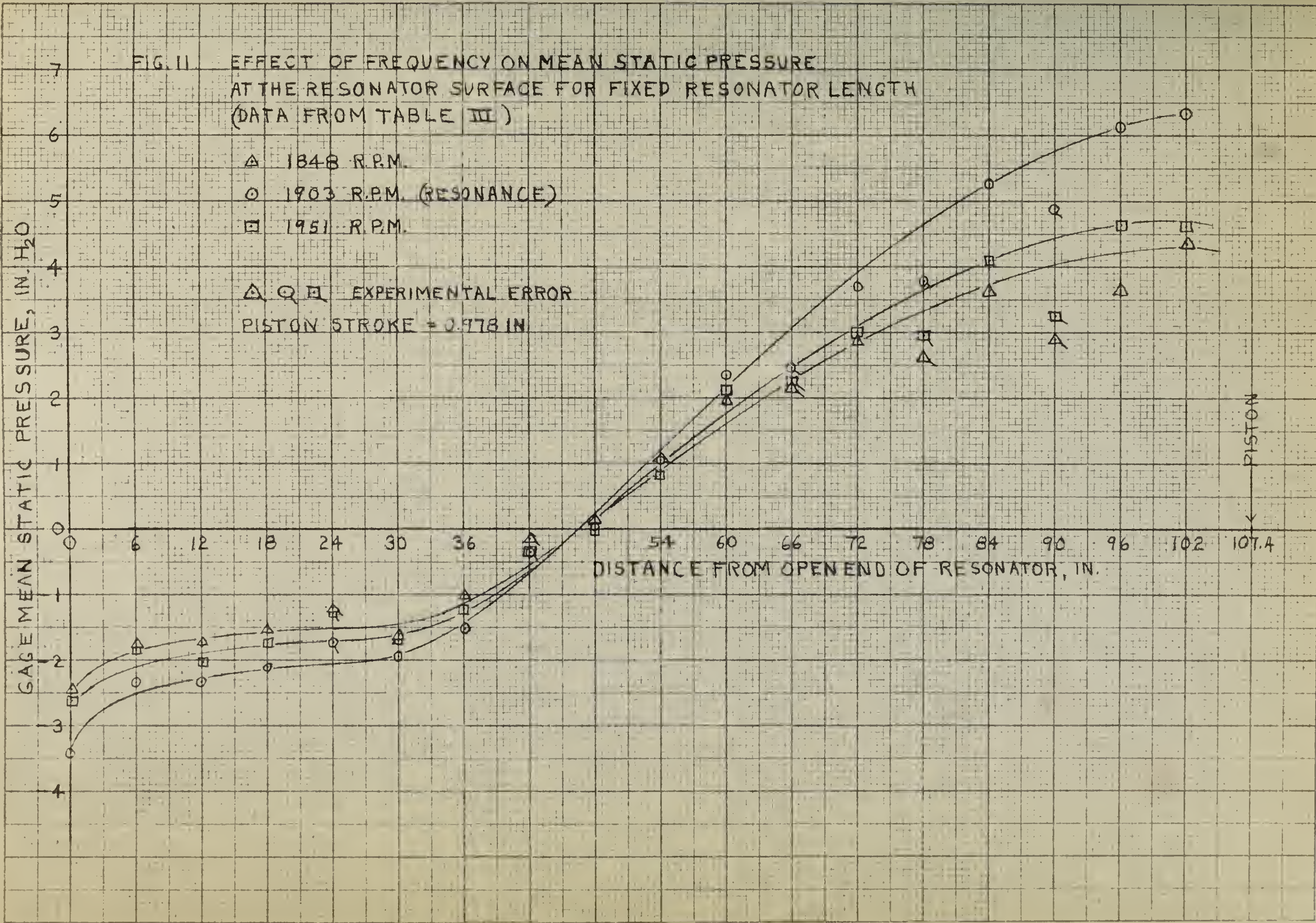

FIG. 11 EFFECT OF FREQUENCY ON MEAN STATIC PRESSURE AT THE RESONATOR SURFACE FOR FIXED RESONATOR LENGTH (DATA FROM TABLE III)

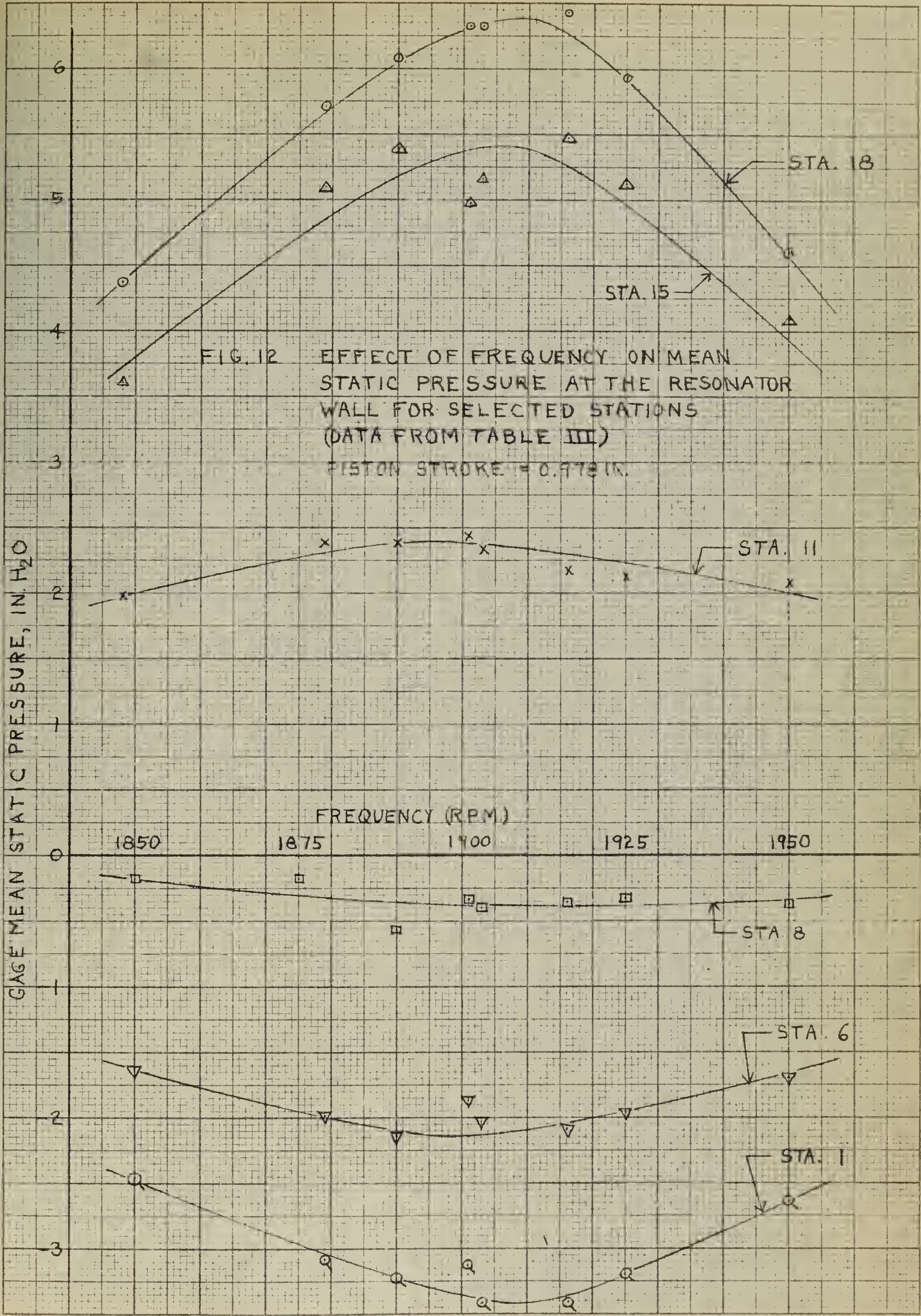

FIG. 12 EFFECT OF FREQUENCY ON MEAN STATIC PRESSURE AT THE RESONATOR WALL FOR SELECTED STATIONS (DATA FROM TABLE III)

PISTON STROKE = 0.972 IN.

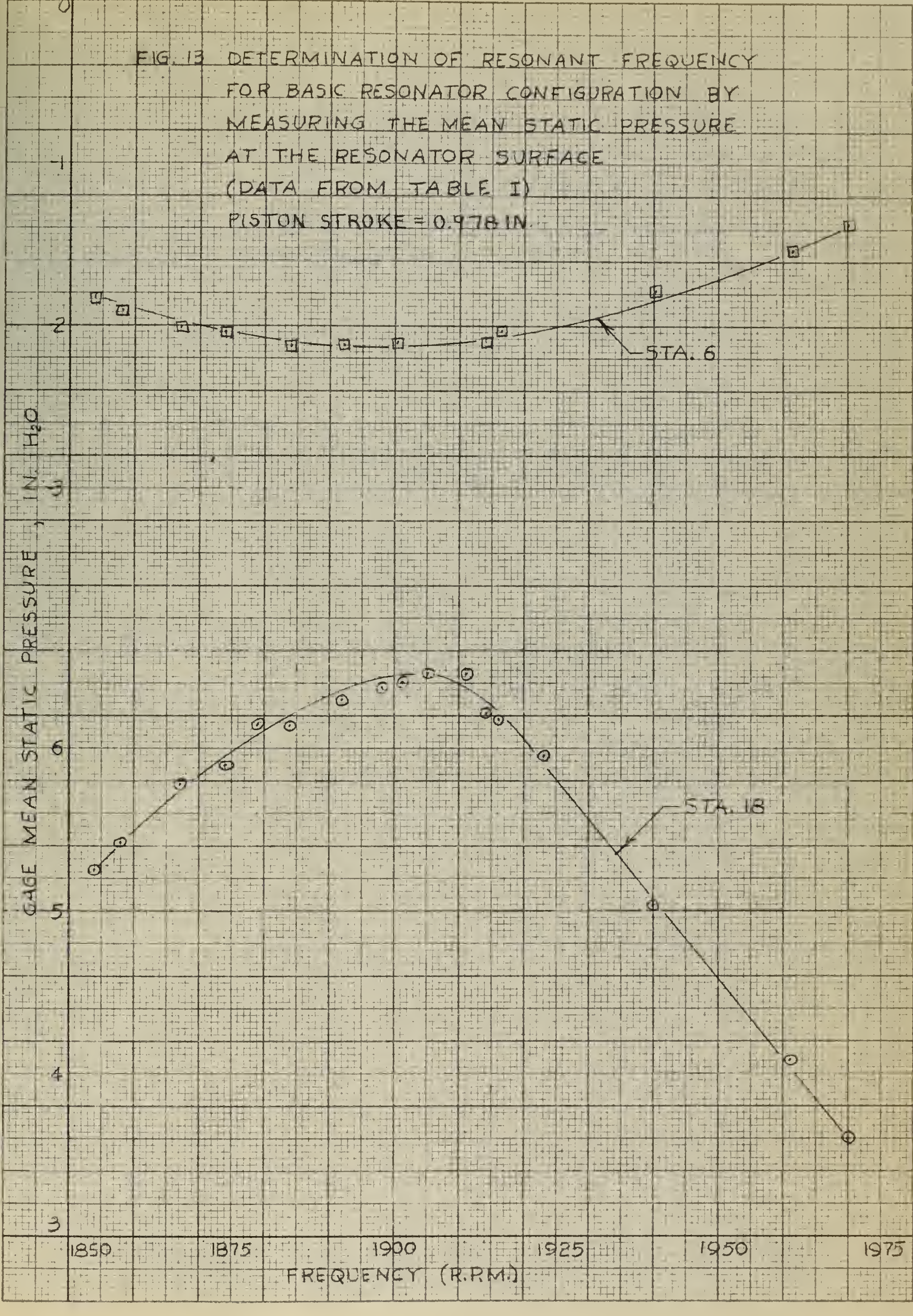

FIG. 13 DETERMINATION OF RESONANT FREQUENCY FOR BASIC RESONATOR CONFIGURATION BY MEASURING THE MEAN STATIC PRESSURE AT THE RESONATOR SURFACE
(DATA FROM TABLE I)
PISTON STROKE = 0.978 IN.

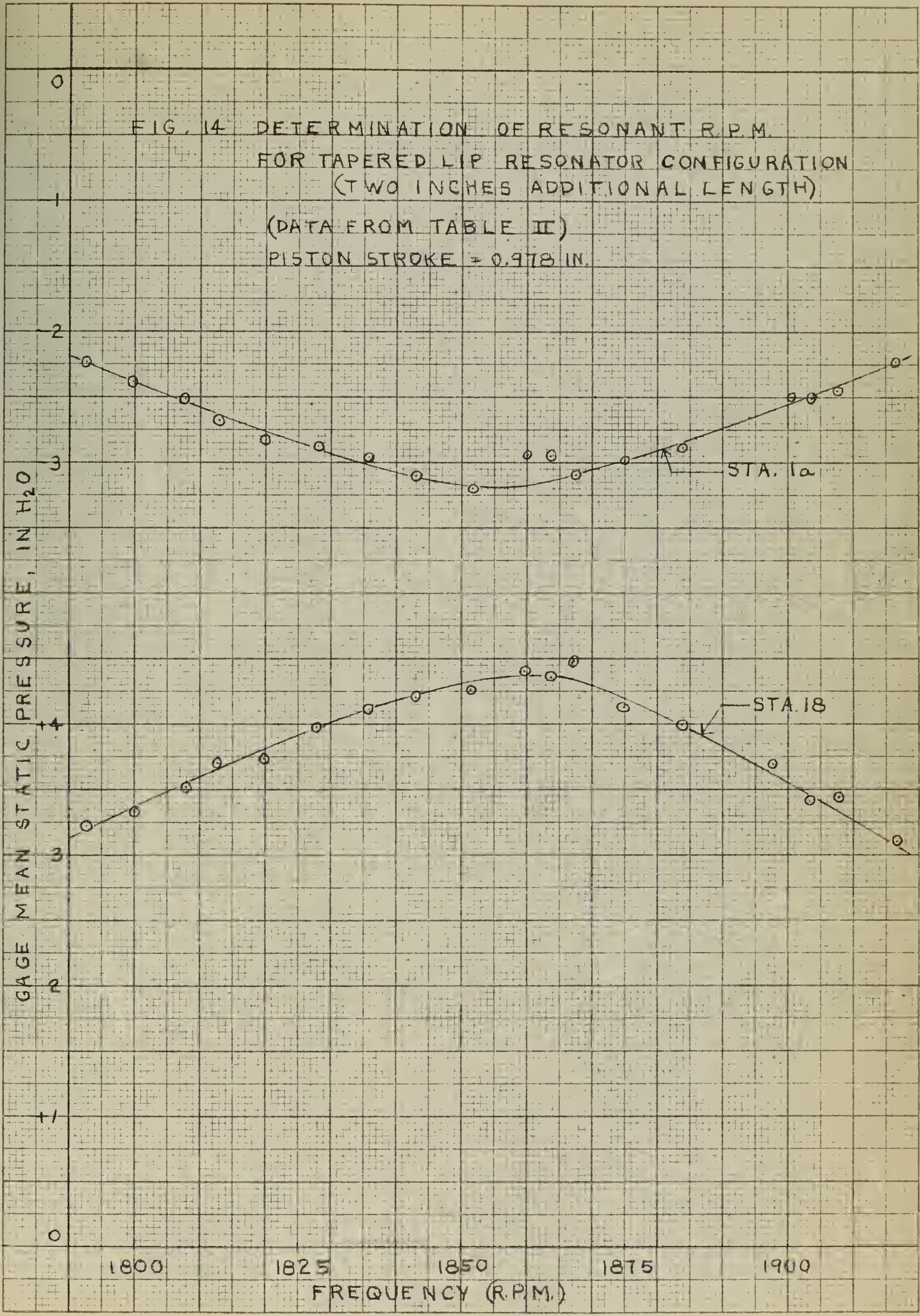
FIG. 14 DETERMINATION OF RESONANT R.P.M.
FOR TAPERED LIP RESONATOR CONFIGURATION
(TWO INCHES ADDITIONAL LENGTH)
(DATA FROM TABLE II)
PISTON STROKE = 0.978 IN.
STA. 1a
STA. 18
GAGE MEAN STATIC PRESSURE, IN H_2O
FREQUENCY (R.P.M.)
1800
1825
1850
1875
1900
0
-1
-2
-3
+4
3
2
+1
0

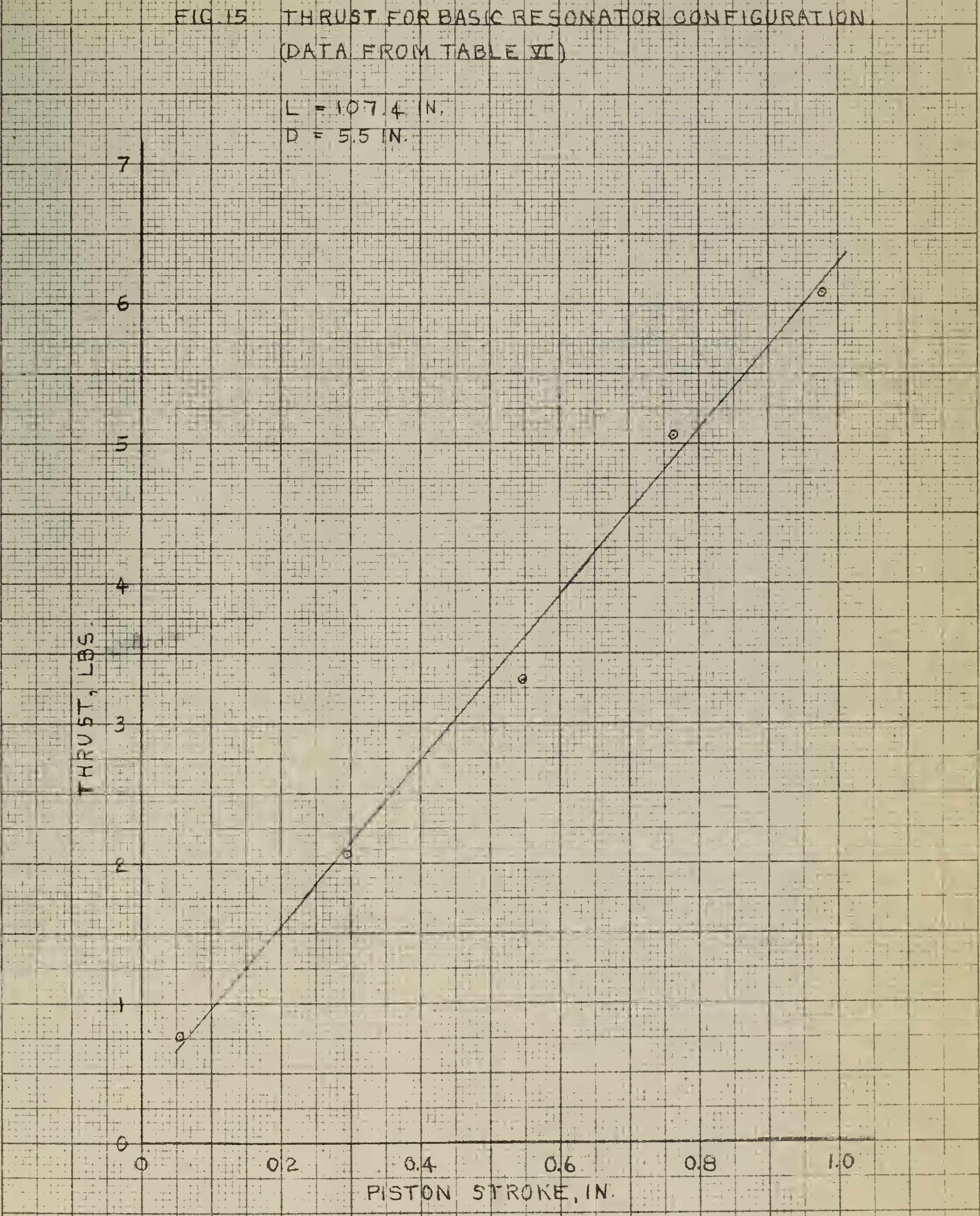
FIG 15 THRUST FOR BASIC RESONATOR CONFIGURATION.
(DATA FROM TABLE VI)
L = 107.4 IN.
D = 5.5 IN.
THRUST, LBS.
PISTON STROKE, IN.
0
1
2
3
4
5
6
7
0.2
0.4
0.6
0.8
1.0

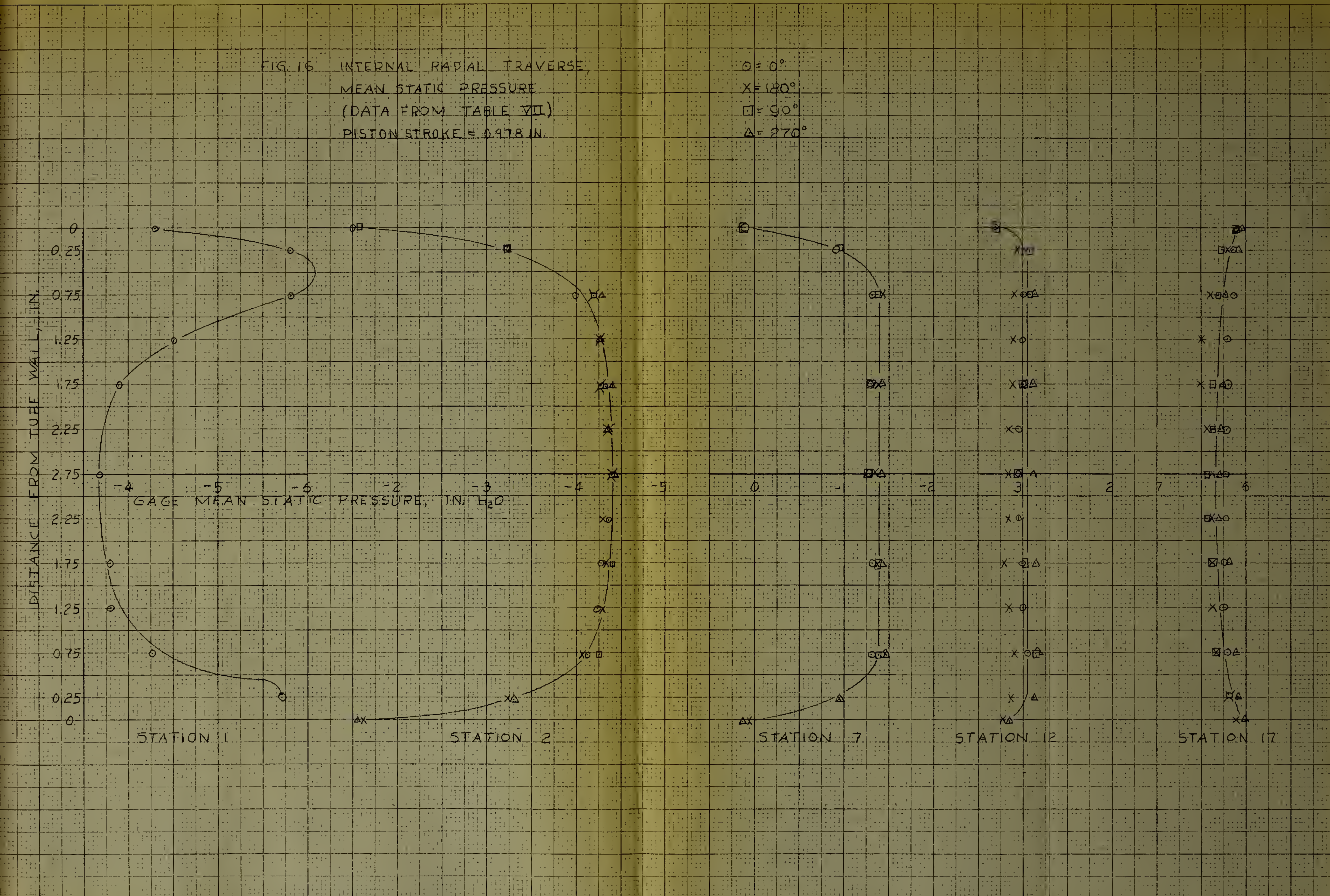

FIG. 16 INTERNAL RADIAL TRAVERSE, MEAN STATIC PRESSURE (DATA FROM TABLE VII) PISTON STROKE = 0.978 IN.
○ = 0°
X = 180°
□ = 90°
△ = 270°
DISTANCE FROM TUBE WALL, IN.
GAGE MEAN STATIC PRESSURE, IN. H_2O
STATION 1
STATION 2
STATION 7
STATION 12
STATION 17

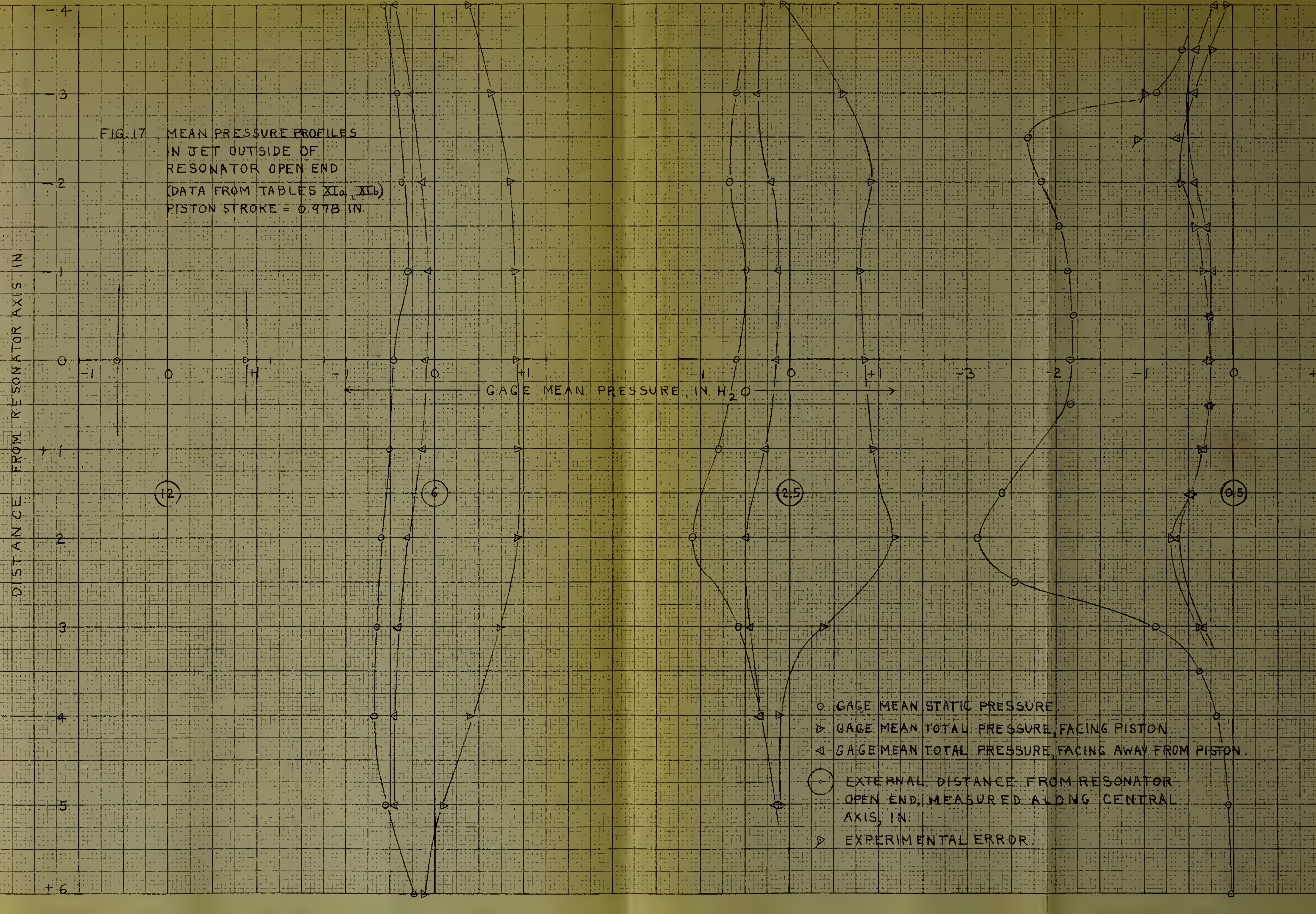
FIG. 17 MEAN PRESSURE PROFILES
IN JET OUTSIDE OF
RESONATOR OPEN END
(DATA FROM TABLES XIa, XIb)
PISTON STROKE = 0.978 IN.
DISTANCE FROM RESONATOR AXIS, IN.
GAGE MEAN PRESSURE, IN. H2O
GAGE MEAN STATIC PRESSURE.
GAGE MEAN TOTAL PRESSURE, FACING PISTON.
GAGE MEAN TOTAL PRESSURE, FACING AWAY FROM PISTON.
EXTERNAL DISTANCE FROM RESONATOR OPEN END, MEASURED ALONG CENTRAL AXIS, IN.
EXPERIMENTAL ERROR.
12
6
2.5
0.5

FIG. 18 INTERNAL RADIAL TRAVERSE
MEAN TOTAL PRESSURE
(DATA FROM TABLE IX)
PISTON STROKE = 0.978 IN.

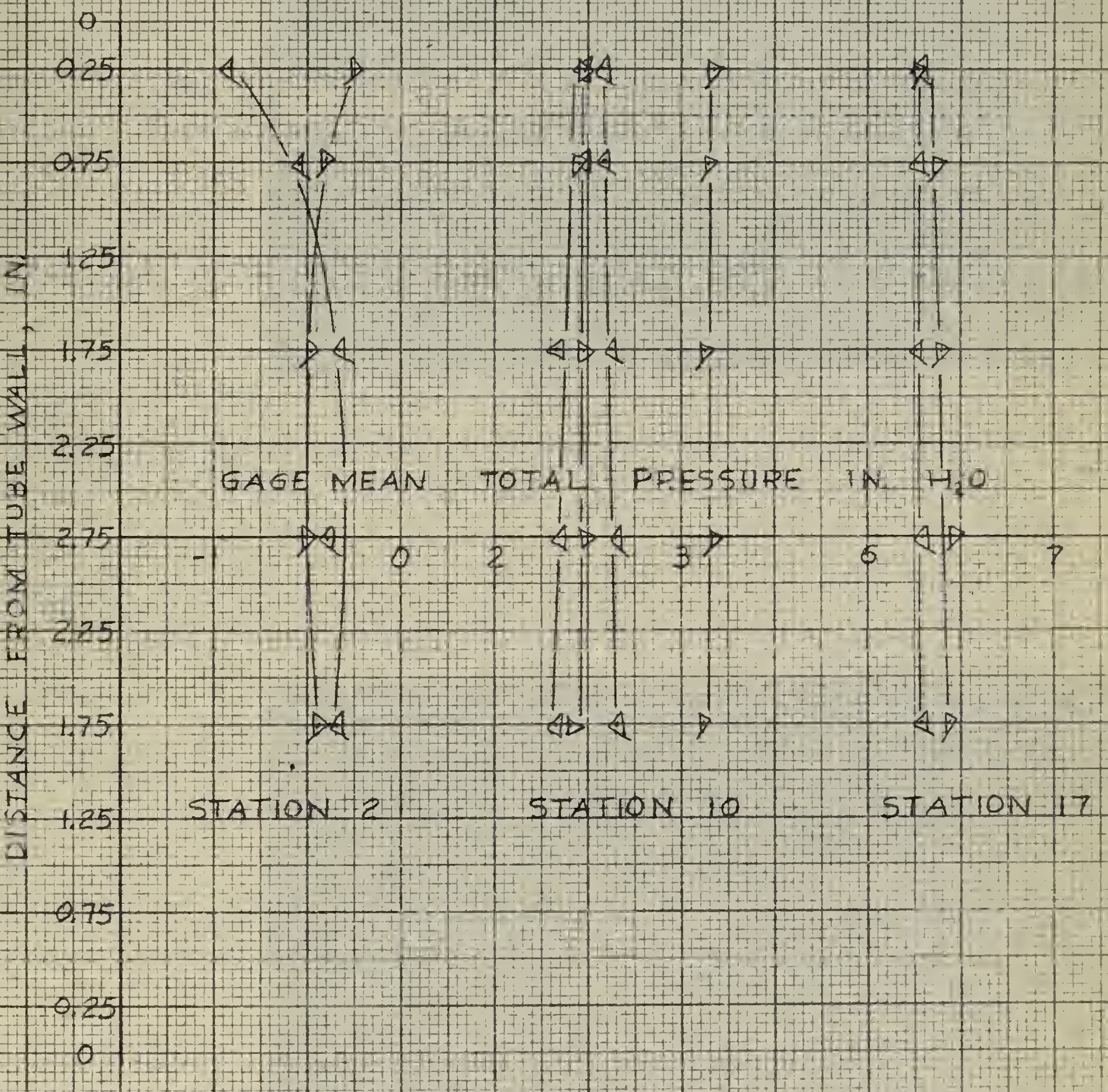

▷ = "L" TYPE TOTAL-HEAD PROBE FACING PISTON
◁ = "L" TYPE TOTAL-HEAD PROBE FACING AWAY FROM PISTON
▷ = CYLINDER TYPE TOTAL-HEAD PROBE FACING PISTON
◁ = CYLINDER TYPE TOTAL-HEAD PROBE FACING AWAY FROM PISTON

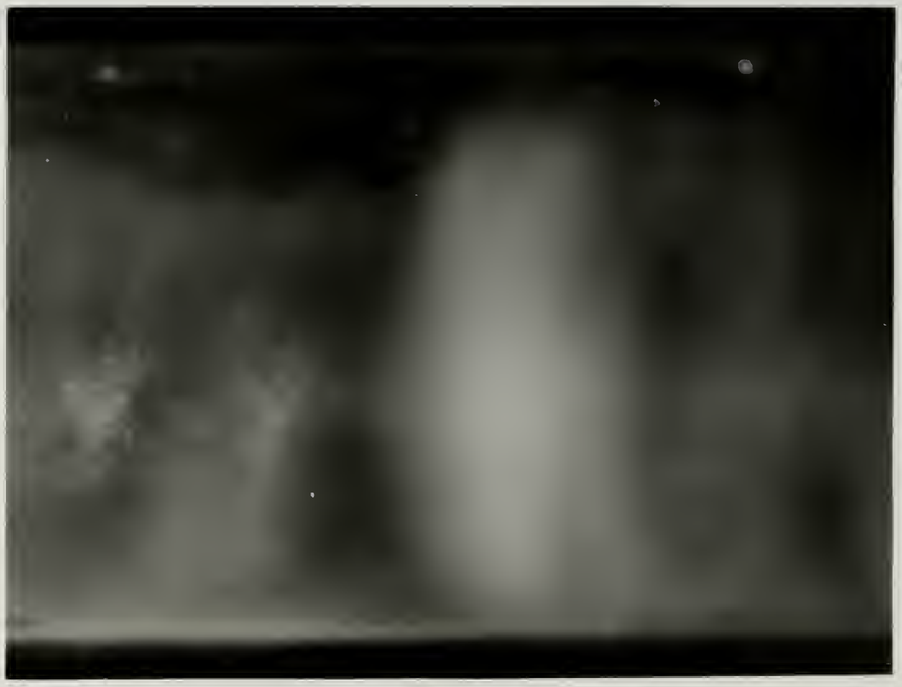

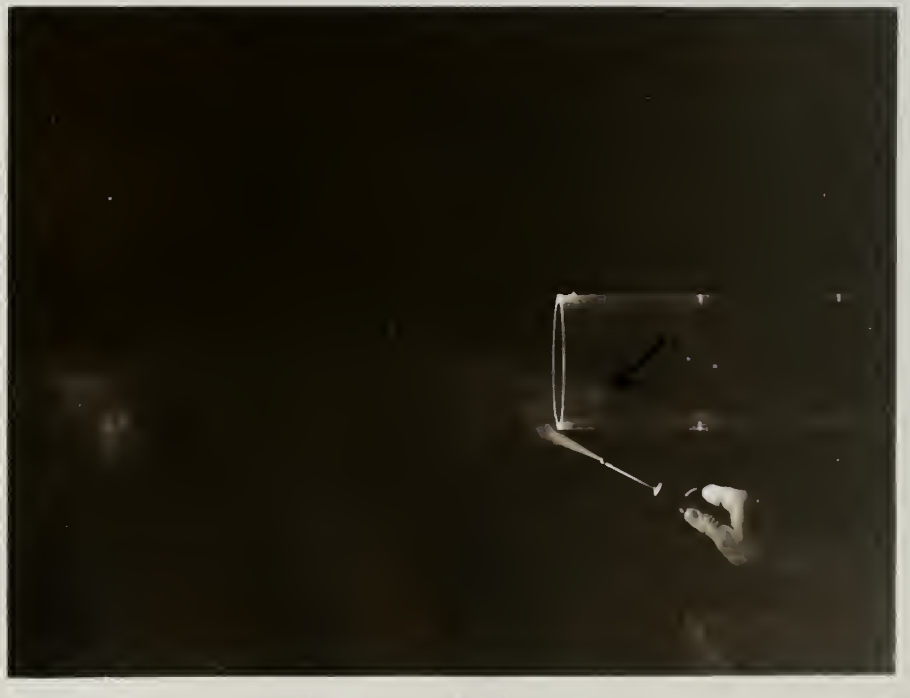

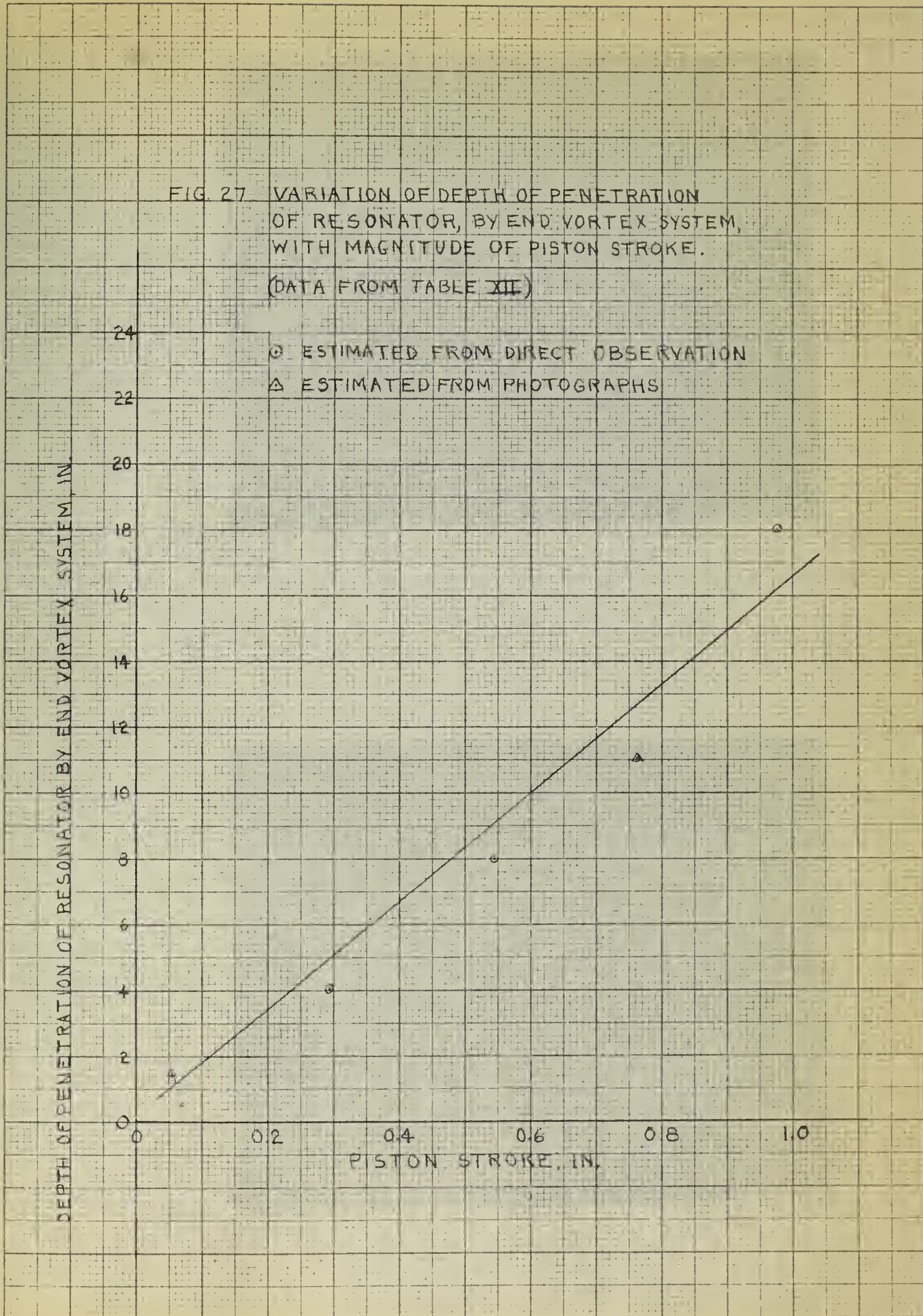
FIG. 27 VARIATION OF DEPTH OF PENETRATION OF RESONATOR, BY END VORTEX SYSTEM, WITH MAGNITUDE OF PISTON STROKE.
(DATA FROM TABLE XII)
⊙ ESTIMATED FROM DIRECT OBSERVATION
△ ESTIMATED FROM PHOTOGRAPHS
DEPTH OF PENETRATION OF RESONATOR BY END VORTEX SYSTEM, IN.
PISTON STROKE, IN.
0
2
4
6
8
10
12
14
16
18
20
22
24
0
0.2
0.4
0.6
0.8
1.0

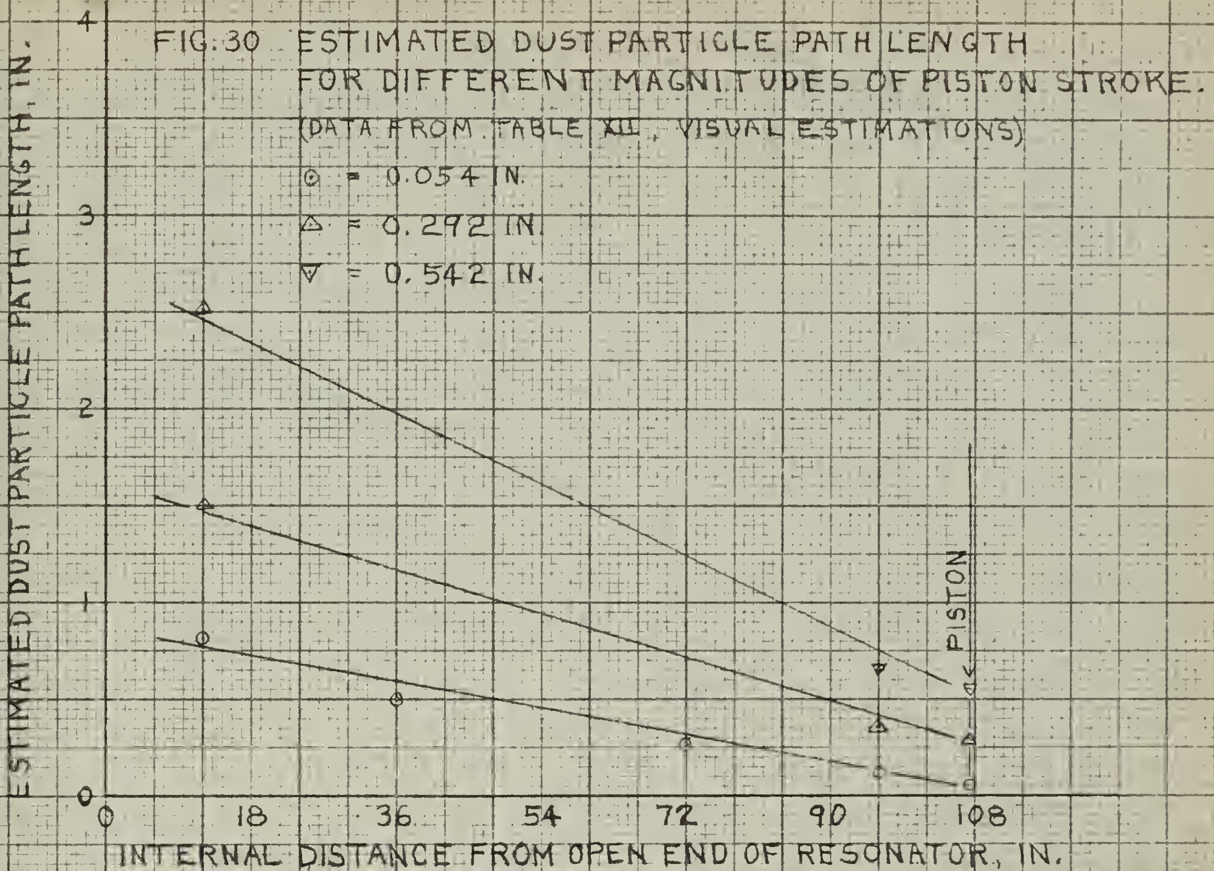

FIG. 30 ESTIMATED DUST PARTICLE PATH LENGTH FOR DIFFERENT MAGNITUDES OF PISTON STROKE.

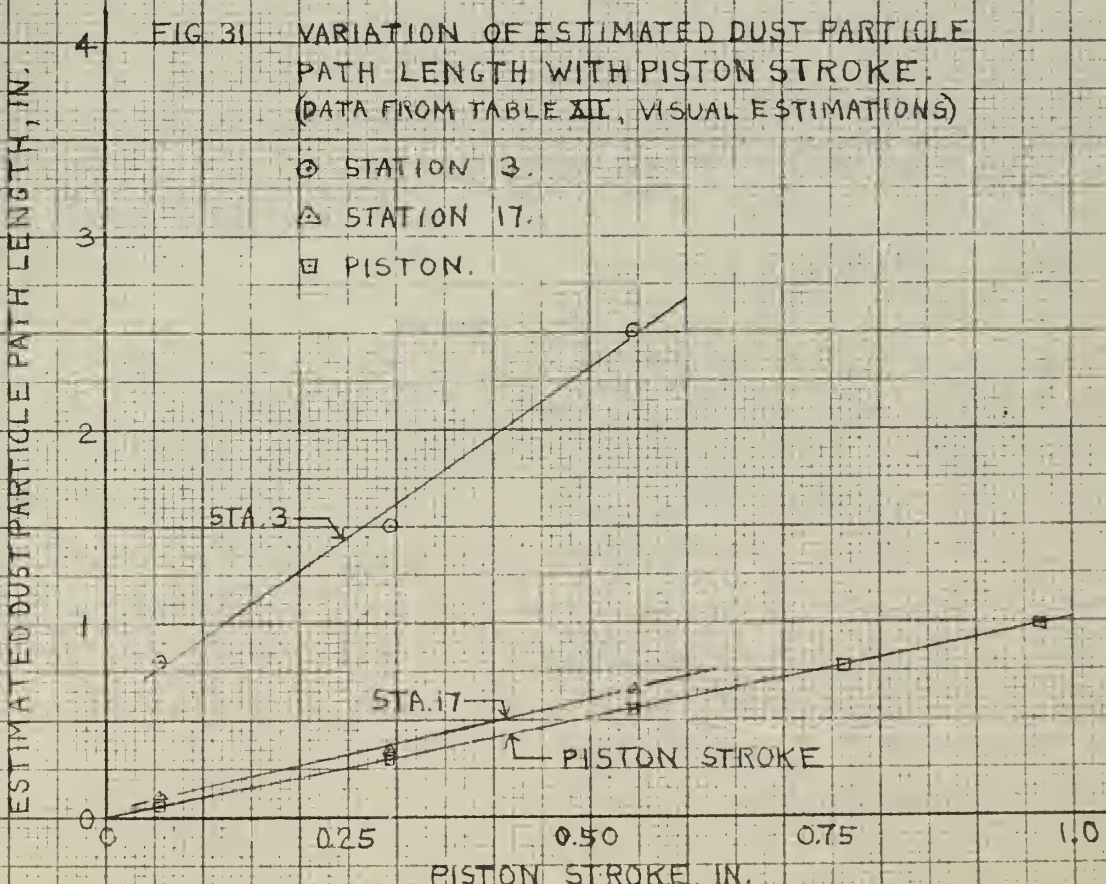

FIG. 31 VARIATION OF ESTIMATED DUST PARTICLE PATH LENGTH WITH PISTON STROKE.

FIG 32 IDEALIZED TIME-DISTANCE DIAGRAM OF WAVE PROGRESS IN A RESONATOR CLOSED AT ONE END BY A PULSATOR AND OPEN AT THE OTHER END

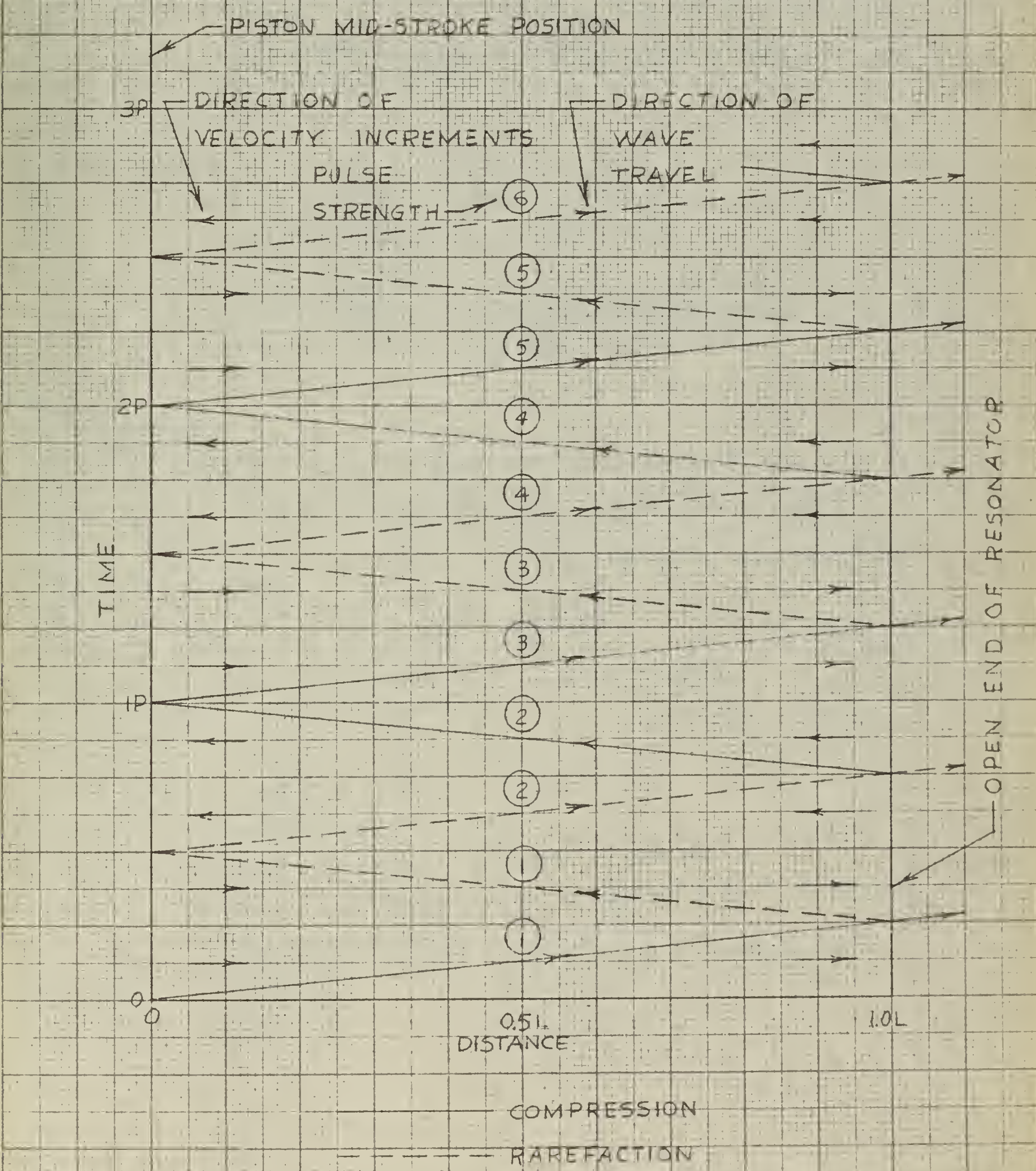

SAMPLE CALCULATIONS

RESONATOR FREQUENCY:

$r = 2.75$ in.; $L = 107.4$ in.; $t = 88°F$ (Table I);

$$f = \frac{12 \cdot 1148}{4[107.4 + 0.6(2.75)]} = 31.63 \text{ c.p.s.} = 1898 \text{ R.P.M.}$$

VELOCITY:

$h_o = -0.67$ in. H_2O (Table X, Sta. 1)

$h_s = -3.68$ in. H_2O (Table VIII, Sta. 1)

$$V = \sqrt{\frac{2(p_o - p_s)}{\rho}} = \sqrt{\frac{2(64.2)(3.68 - 0.67)}{(12)(0.002378)}} = 116 \text{ ft./sec.}$$

THRUST:

$H_a = 29.42$ in. Hg $= 400$ in. H_2O (Table V).

$h_{s(piston)} = h_{s_p} = +6.6$ in. H_2O (Fig. 8, uncorrected)

$h_{s(open\ edge)} = h_{s_e} = -3.6$ in. H_2O (Fig. 8, uncorrected).

$T = p_{s_p} \cdot A_p + p_{s_e} \cdot A_e - p_a \pi(3)^2$

p_{s_p} = absolute pressure on piston, lbs/in.^{2}

p_{s_e} = " " " open-end edge, lbs/in.^{2}

p_a = " " , atmospheric assumed acting externally on unit.

A_p = piston area $= \pi(2.75)^2 = 23.80$ in^2

A_e = open-end edge area $= \pi(3)^2 - A_p = 4.48$ in^2.

$$T = \frac{62.4}{12 \cdot 144}\left[406.6(23.8) + 396.4(4.48) - 400(28.28)\right]$$

$= 6.06$ lbs.

5/9

DATE DUE

Thesis 16259
J28 Janes
Investigation of the air-flow in an acoustic jet a resonance.

Thesis 16259
J28 Janes
Investigation of the air-flow in an acoustic jet a resonance.

thesJ28
Investigation of the air-flow in an acou
3 2768 002 10015 8
DUDLEY KNOX LIBRARY